

UNIVERSIDADE DE LISBOA
FACULDADE DE CIÊNCIAS
DEPARTAMENTO DE FÍSICA



Methodological Study on Diffusion Tensor Indices in MS: Analysis Challenges and Outcomes

Catarina Correia de Freitas

Dissertação

Mestrado Integrado em Engenharia Biomédica e Biofísica

Perfil de Radiações em Diagnóstico e Terapia

2013

UNIVERSIDADE DE LISBOA
FACULDADE DE CIÊNCIAS
DEPARTAMENTO DE FÍSICA



Methodological Study on Diffusion Tensor Indices in MS: Analysis Challenges and Outcomes

Catarina Correia de Freitas

Dissertação

Mestrado Integrado em Engenharia Biomédica e Biofísica

Perfil de Radiações em Diagnóstico e Terapia

Orientador externo: Professora Doutora Claudia Wheeler-Kingshott

Orientador interno: Professora Doutora Rita G. Nunes

2013

Resumo

A imagem de tensor de difusão (ITD) é uma modalidade de ressonância magnética (RM) que permite determinar in vivo a intensidade e a direção da difusão da água nos tecidos biológicos. A mobilidade molecular nos tecidos depende da sua organização celular. Em estruturas organizadas, como na substância branca do cérebro, em que há uma grande compactação de fibras nervosas, a difusão é restringida na direção perpendicular aos axónios e ocorre preferencialmente na direção paralela às fibras. Como esta direcionalidade é observável com a ITD, esta técnica permite concluir acerca da microestrutura dos tecidos e investigar alterações estruturais que ocorrem em caso de patologia. O fato de a ITD proporcionar novos contrastes da estrutura da substância branca comparativamente à imagem de RM convencional, torna-a uma técnica apelativa para inúmeros estudos neurológicos, designadamente, estudos de doenças neurodegenerativas, como a esclerose múltipla (EM).

Na ITD, a difusão em cada voxel é descrita por um tensor que, após diagonalizado, pode ser definido por três valores próprios, λ_1 , λ_2 e λ_3 e os seus correspondentes vetores próprios, v_1 , v_2 e v_3 . Através desta informação, o tensor de difusão (TD) pode ser representado geometricamente como um elipsóide cujos eixos estão alinhados com os vetores próprios e cujas dimensões estão de acordo com a raiz quadrada dos valores próprios. Por sua vez, o maior eixo do elipsóide corresponde à direção principal da difusão, que se assume como sendo paralela à direção das fibras nervosas.

A informação dada pelos tensores pode ser mais facilmente visualizada calculando índices que correspondem a certas propriedades da difusão. Nomeadamente, o primeiro valor próprio define o parâmetro de difusibilidade axial (DA), o qual está associado à difusão na direção das fibras nervosas, e a média do segundo e terceiro valores próprios corresponde ao parâmetro de difusibilidade radial (DR), o qual mede a difusão na direção perpendicular às fibras. Alterações nestes dois parâmetros são associadas, respetivamente, à degeneração axonal e à desmielinização dos neurónios. Outros índices são a difusibilidade média (DM), que corresponde à média dos três valores próprios, e a anisotropia fracional (AF), que mede a direcionalidade da difusão, a qual pode variar entre 0 (isotrópica) e 1 (extremamente direcionada).

No entanto, existem algumas limitações associadas à ITD que dificultam a interpretação dos seus resultados. Em primeiro lugar, o modelo que é utilizado é incapaz

de representar voxels onde ocorre cruzamento de tratos não paralelos de fibras nervosas. Nos restantes casos, fatores como uma baixa razão sinal-ruído e a presença de lesões podem desviar o tensor da direção correta das fibras nervosas. Nestes casos, a comparação de índices de difusão entre diferentes sujeitos pode resultar em conclusões enganadoras, dado que se estão a comparar valores que correspondem às características da difusão ao longo de diferentes estruturas biológicas.

Este projeto teve como objetivo criar e testar uma metodologia, com base no trabalho desenvolvido por Wheeler-Kingshott et al. (2012), para comparar, de forma consistente, a informação dada pelas imagens de TD entre um grupo de indivíduos saudáveis e um grupo de pacientes com EM. Neste método, em cada voxel, os índices de difusão não são calculados diretamente a partir dos valores próprios do TD, mas da projeção dos TD na direção de vetores próprios de referência, que se assumem como estando alinhados com a direção saudável das fibras nervosas. Estes vetores próprios são retirados de uma imagem de TD de referência construída a partir da média de imagens de TD correspondentes aos sujeitos saudáveis da população. No estudo desenvolvido, participaram 48 controlos e 76 doentes com EM.

Para se poder comparar as diferenças entre o grupo de pacientes e o grupo de indivíduos saudáveis, foi primeiro necessário proceder à normalização das imagens de TD. Assim, estas imagens foram alinhadas a um *template* criado a partir de um subconjunto de 20 controlos e 20 pacientes. Para o alinhamento, foram utilizados dois métodos diferentes: um baseado nas próprias imagens de DT e o outro baseado nos mapas escalares de AF dessas imagens e do *template*.

De seguida, foram obtidos os vetores e os valores principais de cada tensor das imagens da população em estudo. Com estes valores principais, foram calculados os índices DA, DR e AF. Foram igualmente calculados os pares de vetores e valores principais para a imagem de referência. Os tensores de cada sujeito foram projetados nas direções de referência, dando origem aos valores principais projetados. Estes últimos foram utilizados para calcular os índices projetados: difusibilidade axial projetada (DAP), difusibilidade radial projetada (DRP) e anisotropia fracional projetada (AFP).

Para cada método de alinhamento utilizado, foi conduzida uma análise estatística para comparar as diferenças detectadas entre o grupo de controlos e o grupo de pacientes usando os índices normais e os índices projectados. Os resultados mostraram que existiu um aumento de DA, DR, DAP e DRP e uma diminuição de AF e AFP nos pacientes em relação aos controlos. A extensão e a localização das alterações entre parâmetros análogos (DA e DAP, DR e DRP, e AF e AFP) foram detetadas de forma muito semelhante, sobrepondo-se em grande parte e diferindo apenas em algumas pequenas zonas. Foram observadas diferenças mais extensas

entre os parâmetros projetados e os parâmetros normais através do método de alinhamento que utilizava os mapas de AF. Contudo, apesar de não terem sido observados resultados conclusivos, foram identificadas algumas diferenças que podem sugerir uma maior sensibilidade dos parâmetros projetados para identificar os elementos patológicos da EM.

As alterações detetadas com os parâmetros normais derivados de ambas as técnicas de alinhamento foram também comparadas, o que mostrou que os resultados podem ser consideravelmente influenciados pela técnica (baseada nos mapas AF ou nas imagens de TD) escolhida para o alinhamento das imagens. Foi também observado que o alinhamento com as imagens de AF é menos eficaz a alinhar os tensores com o *template*. De fato, verificou-se uma maior dispersão na orientação dos tensores do grupo em estudo utilizando esta técnica. No entanto, é necessário investigar qual dos métodos de normalização das imagens de TD é o indicado para efetuar análises comparativas entre pacientes e controlos porque, apesar de o método de TD ser mais eficaz no alinhamento dos tensores, esta reorientação pode porventura cancelar também informações adicionais sobre patologia.

Estudos postmortem deverão ser efetuados de forma a testar o fundamento biológico dos parâmetros projetados comparativamente aos parâmetros normais e também para se investigar qual dos métodos de alinhamento tem maior especificidade e sensibilidade para detetar patologia em estudos comparativos de ITD entre pacientes e controlos.

PALAVRAS-CHAVE: imagem de tensor de difusão, difusibilidade axial projetada, difusibilidade radial projetada, anisotropia fracional projetada, esclerose múltipla, alinhamento com tensor de difusão, alinhamento com anisotropia fracional.

Abstract

Diffusion tensor imaging (DTI) characterizes the diffusion properties of the tissues through a tensor. This tensor can be used to calculate scalar indices that are used to study white matter (WM) changes in several neurological diseases. The diffusion tensor (DT) assigns a principal direction for diffusion that, in the WM of the brain, is assumed to be aligned with the direction of the axonal fibres. However, there are some cases where this supposition fails. As a result, misinterpretation of differences in DT indices between patients and healthy controls (HCs) may occur when the geometrical properties of the datasets are not taken into consideration. To solve this problem, a new analysis method consistent between subjects was introduced. Here, diffusion is measured along reference vectors that define the most probable direction of healthy diffusion. This study aimed to develop a pipeline for the use of this new approach in group comparisons of HCs and patients with multiple sclerosis (MS), and test its sensitivity at identifying pathology compared to the standard approach. This analysis was done using two different registration methods: DT-based and FA-based. In general, it was shown that at a group level there were no major differences between the standard and the projected indices. However, results were observed that could suggest increased sensitivity for the latter. In addition, a significant effect of the registration method was detected in the results. Also, the coherence of tensor's orientation between datasets was studied, which showed that the FA-based registration aligns tensors to a lesser degree than the DT-based. The pipeline developed in this work should be further investigated to enable a final conclusion regarding its validity and sensitivity. Also, additional work should be performed to investigate whether the realignment based on the DTI rather than FA properties may mask pathological processes or viceversa.

KEYWORDS: diffusion tensor imaging, projected axial diffusivity, projected radial diffusivity, projected fractional anisotropy, multiple sclerosis, DT-based registration, FA-based registration.

Acknowledgements

The completion of this dissertation wouldn't have been possible without the support of several people, to whom I would like to express my sincere gratitude.

First of all, I am extremely grateful to my external supervisor Dr. Claudia Wheeler-Kingshott for her help, encouragement and kindness. It as a great opportunity to have worked in IoN, moreover, under her guidance, and to have learned so much with her expertise.

I would like to express my sincere gratitude to my internal supervisor Dr. Rita Nunes, who was always very supportive and helpful. In addition, I am very thankful to both my supervisors for all their patience, critics and comments when correcting my thesis.

I would also like to show my appreciation to the researchers and collaborators in IoN for the friendly work atmosphere. In particular, I thank Dr. Gary Zhang for his kind availability to help and give suggestions to my work.

I gratefully acknowledge the financial support given by the Erasmus Grant and the NMR Research Unit of UCL Institute of Neurology.

In addition, I must thank the "Portuguese Gang" in London for all the companionship, dinner parties and good times. Besides them being great people, it was also very good to have a little bit of home during my stay.

I am also very much indebted to my closest friends for their support and encouragement in the moments where I needed the most.

E por fim, gostaria de agradecer à minha família por todo o apoio que me deram ao longo da minha vida. Agradeço especialmente a dedicação dos meus pais, sem a qual não teria sido possível fazer este trabalho. Agradeço também à minha irmã e aos meus sobrinhos por todo o carinho, palhaçadas e alegria, que foram muito importantes para não perder a motivação durante a escrita da tese.

Contents

| | |
|--|-------------|
| List of Figures | viii |
| List of Tables | ix |
| List of Abbreviations | x |
| 1 Introduction | 1 |
| 1.1 Aim of the work | 1 |
| 1.2 Dissertation outline | 2 |
| 2 Background | 3 |
| 2.1 Measuring diffusion in the brain | 3 |
| 2.2 Diffusion tensor imaging | 6 |
| 2.3 Multiple sclerosis and DTI | 9 |
| 3 Projected DTI indices as new measures to study WM integrity | 13 |
| 3.1 Motivation and objectives | 13 |
| 3.2 Methods | 14 |
| 3.2.1 Data and processing pipeline | 15 |
| 3.2.2 Registration | 17 |
| 3.2.3 Calculation of the DTI indices | 21 |
| 3.2.4 DTI indices statistical analysis | 22 |
| 3.2.5 Angles calculation and analysis | 23 |
| 3.2.6 Creation of the lesion probability map | 24 |
| 3.3 Results | 25 |
| 3.3.1 Statistical analysis | 25 |
| 3.3.2 Angles analysis | 28 |
| 3.4 Discussion | 29 |
| 3.5 Conclusion | 31 |

| | | |
|----------|---|-----------|
| 4 | The effect of registration on VBA of DT-MRI data | 33 |
| 4.1 | Motivation and objectives | 33 |
| 4.2 | Methods | 34 |
| 4.3 | Results | 35 |
| 4.3.1 | Statistical analysis | 35 |
| 4.3.2 | Angles analysis | 38 |
| 4.4 | Discussion | 40 |
| 4.5 | Conclusion | 41 |
| 5 | Conclusions | 43 |
| 5.1 | Summary | 43 |
| 5.2 | Contribution | 43 |
| 5.3 | Future work | 44 |
| 5.4 | Concluding remarks | 44 |
| | Bibliography | 46 |

List of Figures

| | | |
|-----|---|----|
| 2.1 | Diffusion anisotropy in white matter | 4 |
| 2.2 | Schematic of the pulsed field gradient spin-echo Magnetic Resonance (MR) technique introduced by Stejskal and Tanner | 5 |
| 2.3 | Diffusion tensor ellipsoid and its dependence on the structure of physical obstructions | 7 |
| 2.4 | Visualization of the scalar indices Mean Diffusivity (MD) and Fractional Anisotropy (FA) | 8 |
| 3.1 | Importance of tensor reorientation after registration | 18 |
| 3.2 | Template | 20 |
| 3.3 | Schematics of the projected indices calculation | 22 |
| 3.4 | Lesion probability map | 24 |
| 3.5 | Results showing areas with increased PAD in MS patients | 25 |
| 3.6 | Results showing areas with increased PRD in MS patients | 26 |
| 3.7 | Results showing areas with decreased PFA in MS patients | 26 |
| 3.8 | Results of the comparison between the projected and original indices | 27 |
| 3.9 | Results of the angle dispersion analysis between the mean DT-datasets | 29 |
| 4.1 | Results of the comparison between the FA-based and DT-based registration method | 36 |
| 4.2 | Results of the comparison between the projected and original indices obtained with FA-based registration | 37 |
| 4.3 | Results of the angle dispersion analysis between the mean DT-datasets obtained with FA-based registration | 38 |
| 4.4 | Results of the angle dispersion analysis between the mean HC DT-datasets obtained with DT-based pipeline and with FA-based pipeline | 39 |
| 4.5 | Angle analysis histogram | 39 |

List of Tables

| | | |
|-----|---|----|
| 2.1 | Clinical meaning of each Expanded Disability Status Scale (EDSS) score for a patient. | 10 |
| 3.1 | Subject group descriptives (mean±standard deviation). | 15 |
| 3.2 | Template group descriptives (mean±standard deviation) | 19 |
| 4.1 | Percentage of WM voxels with angles above 5 degrees | 40 |

List of Abbreviations

AD Axial Diffusivity

ADC Apparent Diffusion Coefficient

BET Brain Extraction Tool

CNS Central Nervous System

DD Disease Duration

DT Diffusion Tensor

DTI Diffusion Tensor Imaging

DW Diffusion-Weighted

DWI Diffusion-Weighted Imaging

EDSS Expanded Disability Status Scale

FA Fractional Anisotropy

HCS Healthy Controls

LPM Lesion Probability Map

MD Mean Diffusivity

MR Magnetic Resonance

MRI Magnetic Resonance Imaging

MS Multiple Sclerosis

NAGM Normal-Appearing Gray Matter

NAWM Normal-Appearing White Matter

PAD Projected Axial Diffusivity

PFA Projected Fractional Anisotropy

PP Primary Progressive

PPD Preservation of Principal Directions

PR Progressive-Relapsing

PRD Projected Radial Diffusivity

RD Radial Diffusivity

RF Radio-Frequency

ROI Region of Interest

RR Relapsing-Remitting

SNR Signal-to-Noise Ratio

SP Secondary Progressive

SPD Symmetric Positive-Definite

TE Echo Time

TR Repetition Time

VBA Voxel-Based Analysis

WM White Matter

Chapter 1

Introduction

1.1 Aim of the work

Diffusion Tensor Imaging (DTI) is an Magnetic Resonance Imaging (MRI) modality that has emerged as an important new technique for characterizing White Matter (WM) microstructure in health and disease. Since damage in the tissue can affect water diffusion, this technique is able to provide in vivo information about the responsible pathological processes. Additionally, in neurodegenerative diseases as Multiple Sclerosis (MS), DTI can present a higher sensitivity and specificity at detecting abnormal regions in brain white matter compared to conventional MRI.

In DTI, each voxel is defined by a tensor aligned with the main direction of diffusion, which is assumed to be parallel to the axonal fibres. From the tensors, scalar parameters that describe the magnitude and orientation of diffusion can be calculated. When compared between patients and controls, these parameters allow to spatially localize group differences, like alterations in myelin sheath or in cell membrane integrity.

However, misinterpretation of these changes may occur when the alignment of the tensors with the underlying tissue structure is not verified. Factors like a low Signal-to-Noise Ratio (SNR) and the presence of pathology can affect the calculation of the principle direction of diffusivity, deviating the tensor from the true direction of the fibre bundle. In these cases, a comparison between DTI indices of different subjects is not coherent because the tensors represent properties of diffusion along distinct structures.

To solve this problem, a new method for performing DTI quantitative analysis was introduced, which measures diffusion along reference directions derived from Healthy Controls (HCs) [1].

This work aimed to develop and validate a pipeline for this new approach and to assess whether it can be more informative than the standard one at identifying

brain WM changes in a group comparison of controls and MS patients.

In order to achieve this, this project considered two different methods of preparing data for the analysis and hence this dissertation is divided into two parts.

In addition, the overall purpose of this research is to contribute to an accurate assessment of MS microstructural changes. This, in turn, will lead to an improved monitoring of the patients, in a better prediction of the course of the disease, and in the development of new treatments and therapies.

1.2 Dissertation outline

The rest of this dissertation is organized as follows. In the next chapter, important notions regarding this work are addressed, including the concepts of DTI, a brief introduction to MS pathology and a review of imaging analyses on MS. Chapter 3 describes the methodology followed in the first part of this work, shows the results obtained and presents the developed discussion and conclusions. In Chapter 4, the methods, results, discussion and conclusions of the second part of this study are detailed. Finally, Chapter 5 summarizes the results and final conclusions of this research and presents suggestions for future work.

Chapter 2

Background

2.1 Measuring diffusion in the brain

Diffusion

Diffusion is a mass transport process that results from the thermally driven random motion of particles in a fluid, called Brownian motion [2]. At a temperature of absolute zero (0 K) there is no diffusion, however, as the temperature increases, the molecules start vibrating and colliding with each other, which leads to their translational movement [3].

The mean-squared displacement ($\langle x^2 \rangle$) of a diffusing particle over a certain time interval (Δt) depends on a physical constant called diffusion coefficient (D). The equation that describes this relationship (considering the case of free diffusion) was derived by Einstein and is presented below:

$$\langle x^2 \rangle = 2D\Delta t \quad (2.1)$$

The diffusion coefficient is affected by the molecular weight of the particles and by the viscosity and temperature of the media [2, 4].

When there are no barriers to diffusion or in a medium where the restrictions are not geometrically coherent, the molecular mobility is identical in all directions and is called isotropic diffusion. However, if diffusion depends on direction, like in a medium with highly oriented obstructions, it is termed anisotropic.

Diffusion in the brain

In the biological tissues, water mobility is conditioned by the underlying tissue microstructure: by the size, shape and composition of any physical barriers; by the spacing between these hindrances; and also by the permeability of the cellular membrane [5, 6].

In the WM of the brain, which has a very organized microstructure due to the dense packing of the axonal fibres, diffusion is anisotropic. Water is free to diffuse along the direction of the neuronal fibres, both intra and extra-cellularly, but in the perpendicular direction, diffusion is restricted by the cellular membrane and the myelin sheath of the axons (Figure 2.1) [7].

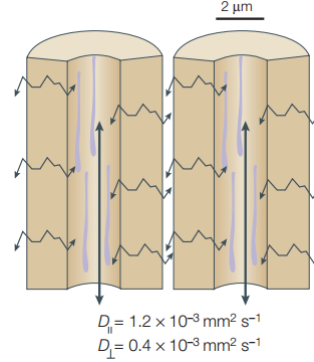


Figure 2.1: Diffusion anisotropy in white matter. Both in the intra-axonal and in the interstitial spaces there is greater hindrance to the molecular displacement along the perpendicular direction (D_{\perp}) of the fibres than along the parallel direction ($D_{||}$). Image adapted from [8].

However, conditions such as trauma, pathology and ageing, can destruct or disarrange the axonal organization, causing a reduction in the anisotropy of diffusion.

Therefore, by studying the diffusivity properties of the neural tissue it is possible to gain insight into the complex structural organization of brain WM and to study the changes that occur due to natural or pathologic physiological processes.

MRI sensitized to diffusion

MRI is based upon the interaction between an applied magnetic field and nuclei that possess spin. In clinical MR imaging, the most used nuclei is the hydrogen.

When exposed to an external magnetic field (B_0), the spinning nuclei start to precess with a frequency proportional to the strength of the applied field, according to the Larmor equation:

$$\omega = \gamma B_0 \quad (2.2)$$

where (ω) is the precessional frequency of the spins (also called Larmor frequency) and γ is the proton gyromagnetic ratio, which is a constant for every atom at a particular magnetic field strength.

In conventional MRI, a homogeneous B_0 is used. However, to sensitize the MR signal to diffusion, diffusion-weighting gradient pulses need to be introduced in the

MR acquisition sequences. The MRI modality that employs this technique is called Diffusion-Weighted Imaging (DWI).

When a gradient pulse is added, it linearly alters the strength of the B_0 field along the applied gradient axis. Accordingly with the Larmor equation, this change will also affect the precessional frequency of the spins [9].

Applying a linear inhomogeneity in the magnetic field makes the spins resonate at different frequencies, depending on the strength of the magnetic field by which they are being affected. At the end of the gradient application, the protons will go back to resonating at the same frequency associated with the B_0 field. However, the same doesn't happen to their phases, which is no longer identical (spins with slightly higher Larmor frequency will accumulate a greater phase). Provided the protons do not move, this dephasing can be reversed by the application of a second gradient, with opposite polarity and with the same strength and length of the first [9].

Yet, this does not happen in the presence of water motion, because the movement of protons between the two gradient pulses leads to imperfect rephasing, and consequently, to signal loss. In this way, the MR image is sensitized to diffusion along the axis of the applied gradients [9].

The image acquisition is generally performed using the Stejskal–Tanner sequence module illustrated in Figure 2.2 [4]. In this scheme, the gradients are applied in the form of rectangular pulses that are inserted in the dephasing and rephasing parts of the spin-echo module. Motion along the gradient axis results in a signal loss proportional to the displacement [10].

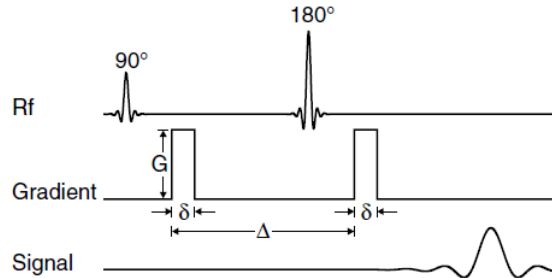


Figure 2.2: Schematic of the pulsed field gradient spin-echo MR technique introduced by Stejskal and Tanner. G and δ correspond to the magnitude and width of the diffusion gradients, respectively; and Δ to the time interval between corresponding points of the two diffusion gradient pulses. Image adapted from [11].

Using this echo scheme, the decreased signal (S) can be compared with the original signal (S_0), using the following equation, that assumes Gaussian diffusion:

$$S = S_0 e^{-\gamma^2 G^2 \delta^2 \left(\Delta - \frac{\delta}{3} \right) ADC} \quad (2.3)$$

Where the Apparent Diffusion Coefficient (ADC) parameter measures the magnitude of diffusion; γ corresponds to the proton gyromagnetic ratio; G and δ to the magnitude and width of the diffusion gradients, respectively; and Δ to the time interval between corresponding points of the two diffusion gradient pulses [12]. By solving this equation, an ADC map can be obtained where the intensity of each voxel is proportional to the rate of water mobility in that voxel.

Moreover, this expression can be simplified using the b value, which characterizes the strength of the applied diffusion-weighting:

$$b = \gamma^2 G^2 \delta^2 \left(\Delta - \frac{\delta}{3} \right) \quad (2.4)$$

However, the use of a scalar (ADC) fails to describe the properties of ordered tissues, such as brain WM and skeletal muscle, where diffusion is anisotropic. In these cases, the ADC maps vary according to the direction of the applied magnetic field gradient.

For this reason, the DWI modality is only used to describe diffusion in isotropic media, where the rate of water mobility is identical in all directions.

In anisotropic media, diffusion needs to be characterized three-dimensionally. This is done using DTI, which uses a tensor to represent the anisotropic nature of diffusion.

2.2 Diffusion tensor imaging

DT model

In DTI, diffusion is characterized by a tensor (\mathbf{D}) instead of a single scalar. The Diffusion Tensor (DT) is a 3x3 Symmetric Positive-Definite (SPD) matrix. Its diagonal elements describe the molecular mobility along the three orthogonal axes of the scanner measurement frame whereas the off-diagonal elements correspond to the correlation between displacements along these axes [11]. The DT is presented below:

$$\mathbf{D} = \begin{bmatrix} D_{xx} & D_{xy} & D_{xz} \\ D_{xy} & D_{yy} & D_{yz} \\ D_{xz} & D_{yz} & D_{zz} \end{bmatrix}$$

Using the DT model, Eq. 2.3 is replaced by the following expression [12]:

$$S_k = S_0 e^{-b \mathbf{g}_k^T \mathbf{D} \mathbf{g}_k} \quad (2.5)$$

Where k varies from 1 to n , and n is the number of applied gradients; S_k is the signal intensity measured after the application of the k_{th} gradient in the \mathbf{g}_k direction;

and S_0 is the original image intensity, measured with no diffusion gradients. The product $\mathbf{g}_k^T \mathbf{D} \mathbf{g}_k$ represents the diffusivity along the direction \mathbf{g}_k .

Eq. 2.5 corresponds to a system of equations that is solved for \mathbf{D} , the diffusion tensor. Since it has 6 independent elements, it is necessary to have at least 7 images to estimate it: 6 Diffusion-Weighted (DW) images acquired with gradients applied in 6 linearly independent directions (giving values for S_1, \dots, S_6) plus one image with no diffusion-weighting (giving the value for S_0). Typically, a much greater number of images is acquired and then a multivariate linear regression is used to fit a tensor to the data.

In DT analysis, the tensor is diagonalized, yielding three pairs of orthogonal eigenvectors (v_1 , v_2 , and v_3) and positive eigenvalues (λ_1 , λ_2 , and λ_3). The eigenvectors are associated with the principal axes of diffusion, whereas the eigenvalues correspond to the diffusion coefficients along the corresponding axis. Additionally, the eigenvectors are sorted according to the descending order of their eigenvalues, so that, at each voxel, the eigenvector correspondent to the largest eigenvalue represents the principal direction of diffusion [13].

Using the eigenvectors and the eigenvalues, the DT can be visually represented by a diffusion displacement-probability ellipsoid (Figure 2.3-A). The ellipsoid represents the distance that a molecule will diffuse from the origin, with equal probability for all the possible directions. The principal axes of the ellipsoid are given by the eigenvectors, and the lengths are scaled according to the square roots of the corresponding eigenvalues [11].

The ellipsoid shape reflects the anisotropy of diffusion. This can be observed in Figure 2.3-B,C.

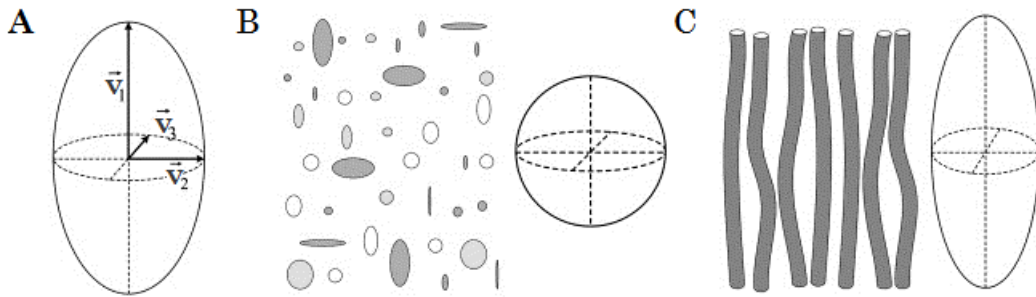


Figure 2.3: Diffusion tensor ellipsoid and its dependence on the structure of physical obstructions. **A** - Diffusion tensor ellipsoid. **B** – In an isotropic tissue, the ellipsoid is spherical. **C** – In coherently organized tissues, diffusion is anisotropic. Image adapted from [14].

DTI scalar indices

The DT eigenvalues can be combined to define several quantitative scalar indices that characterize diffusion magnitude and anisotropy. The simplest scalar that measures the diffusion magnitude is the average of the tensor's eigenvalues [15]. This average is referred to as Mean Diffusivity (MD), which corresponds to the total amount of diffusion in a voxel:

$$MD = \frac{\lambda_1 + \lambda_2 + \lambda_3}{3} \quad (2.6)$$

The anisotropy measures are used to quantify the shape of the diffusion, and consequently, to describe the amount of tissue organization [15]. The most widely used anisotropy measure is the Fractional Anisotropy (FA):

$$FA = \frac{1}{\sqrt{2}} \frac{\sqrt{(\lambda_1 - \lambda_2)^2 + (\lambda_2 - \lambda_3)^2 + (\lambda_1 - \lambda_3)^2}}{\sqrt{\lambda_1^2 + \lambda_2^2 + \lambda_3^2}} \quad (2.7)$$

This index is scaled from 0 (isotropic diffusion) to 1 (highly directional diffusion) and is often considered a measure of white matter integrity.

Other diffusion measures are the Axial Diffusivity (AD) and the Radial Diffusivity (RD). The AD, also called parallel diffusivity, is equal to the largest eigenvalue (λ_1). The RD, also called perpendicular diffusivity, equals the average of the two smaller eigenvalues (λ_2 and λ_3). These measures are interpreted as the diffusivity parallel to and perpendicular to the fibre tracts [15].

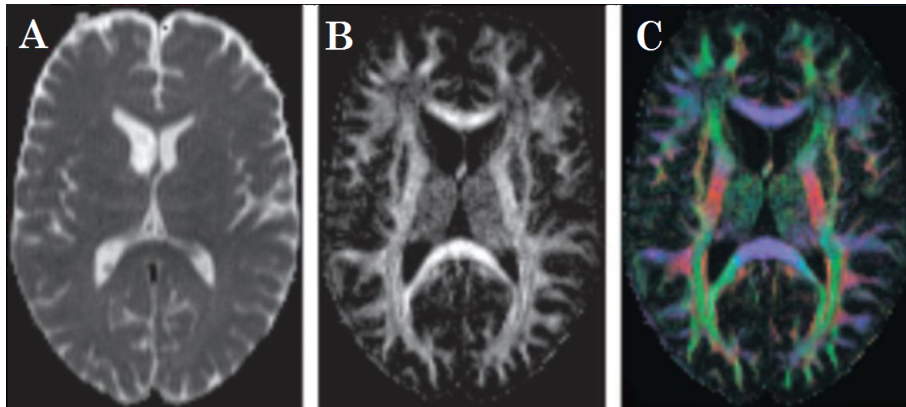


Figure 2.4: Visualization of the scalar indices MD and FA. **A** – MD map; **B** – FA map; **C** – FA image with color coding according to the principal direction of diffusion: in this image, red corresponds to diffusion along the inferior-superior axis; blue to diffusion along the transverse axis; and green to diffusion along the anterior-posterior axis. Image adapted from [16].

These scalar indices can be used for visualizing the diffusion tensor data. In Figure 2.4, MD (A) and FA (B) maps are exemplified. In addition, it is possible to use color coding in the FA maps according to the principal direction of diffusion, as is illustrated in Figure 2.4-C.

The DTI indices can be used probe the integrity of the brain white matter. MD, FA, AD and RD are all very popular indices not only because of their straight forward interpretation in terms of tissue characteristics, but also because they are rotationally invariant, which means that they reflect tissue geometrical properties independently of the relative position of the tissue in the scanner frame of reference and the diffusion weighting directions chosen.

Applications

DTI has been extensively used in neurological studies to quantify the changes of several brain conditions, including white matter diseases, neuropsychiatric conditions, neurodevelopment and aging [17]. These studies are usually conducted by statistically comparing the DTI indices between two or more groups of subjects. This allows to identify what are the diffusion properties that distinguish the different groups which, in turn, can be used to investigate the biological substrate for these differences.

In addition, other important application of DTI is the three-dimensional reconstruction of the white matter tracts, which can be used to represent and measure the structural connectivity in human brains.

Limitations

Despite the promise of this imaging method, the clinical utility of DTI is limited by some factors, such as its dependency on noise and on the inaccurate assumption that water molecules obey Gaussian diffusion in biological tissues [18]. However, the major limitation of DTI is that independently of the tissue architecture, the diffusion properties of each voxel are always averaged by a single diffusion ellipsoid. Therefore, the DT model fails to describe the information of voxels that contain multiple fibres with different orientations.

2.3 Multiple sclerosis and DTI

Multiple sclerosis is a disease in which the immune system attacks the Central Nervous System (CNS), causing the demyelination and sometimes damage of the nervous fibres.

The myelin is an electrically insulating fatty substance that surrounds the nerve fibres and serves the purpose of quickly and efficiently conducting the nervous' impulses along the axons.

When myelin or nerve fibre damage occurs, the electrical signals transmitted throughout the brain and spinal cord are disrupted or distorted. As a consequence, the clinical symptoms of the disease can include loss of motor, cognitive, sensory and visual functions, depending on which nerves are affected [19].

The clinical condition of MS patients is classified according to the Expanded Disability Status Scale (EDSS) score. This is a standard rating system that varies from 0 to 10, quantifying the neurological impairment of MS patients. The clinical meaning of the rating system is described in Table 2.1 [20].

Table 2.1: Clinical meaning of each EDSS score for a patient.

| EDSS score | Neurological impairment |
|------------|--|
| 0.0 | Normal neurological examination |
| 1.0 | No disability |
| 2.0 | Minimal disability |
| 3.0 | Moderate disability |
| 4.0 | Relatively severe disability |
| 5.0 | Disability prevent full daily activities |
| 6.0 | Assistance required to walk |
| 7.0 | Restricted to a wheelchair |
| 8.0 | Restricted to a bed or chair |
| 9.0 | Confined to bed |
| 10.0 | Death |

The primary cause of the disease is unknown, but it is thought to be triggered by genetic and environmental factors. Although currently there is no known cure for MS, medication exists to improve the patient's quality of life by managing the symptoms and controlling the disease course [19].

The manifestation of MS greatly varies from patient to patient. However, there are four major different disease courses that can be distinguished: Relapsing-Remitting (RR); Secondary Progressive (SP); Primary Progressive (PP); and Progressive-Relapsing (PR)) MS [19].

The RR course is the most common MS clinical pattern (about 85% of patients are diagnosed with this type of MS). It is marked by worsening intervals of the neurologic function (relapses) and by intervals of recovery (remissions), in which there is no disease progression. The remitting periods of the disease are a result of axonal and myelin regeneration or resolution of inflammation. The SP type of

MS occurs as an evolution of RR MS (approximately 85% of the RR MS cases evolve to the SP pattern) and is characterized by a steady progress of the disease. Finally, both PP and PR courses are distinguished by a progressive worsening of the condition from the beginning, however, in the latter, punctual attacks of worsening neurologic function occur over time [19,21].

There is no ultimate diagnostic tool for MS. The disease is diagnosed based on the analysis of the clinical symptoms and medical history of the patient along with results from tests that include an MRI of the brain and spinal cord. Due to being a non-invasive technique and to its sensitivity for identifying demyelinating lesions, MRI is the preferred imaging method to help diagnosing MS, to monitor the course of the disease and to control the response to treatment effects [18,19,22].

However, conventional MRI is also limited by low sensitivity to damage in areas of Normal-Appearing White Matter (NAWM) and Normal-Appearing Gray Matter (NAGM) [18] and low pathological specificity to the heterogeneous features of MS pathology [23], which include, for example, the presence and extension of edema, demyelination, axonal injury, and remyelination [18,23]. In addition, this lack of specificity contributes to another limitation of MRI, which is the poor association of the MRI results with the patient's clinical manifestation of the disease [18,23].

Other quantitative MR-based techniques, like diffusion tensor MRI, have the potential to overcome such limitations and contribute to explain the mechanisms that underlie MS pathology.

The different pathologic elements of MS can alter the permeability or geometry of the structural barriers to water diffusion in the brain, which can be depicted by DTI. In general, MS patients have an increased amount of water diffusion and a decreased anisotropy in the region of the lesions, in the surrounding lesion tissue, in the NAWM and in the NAGM. Moreover, these changes seem to be dependent on the clinical course of the patient, since they are found to be greater in patients presenting a more severe course of the disease than in less severe courses [24].

Additionally, in a mice study by Song et al., axonal damage was linked with a decrease in AD, and demyelination with a increase in RD [25,26]. Since then, a lot of studies have focused on analysing these two parameters as potential differentiators between myelin loss and axonal injury. However, although RD, FA and MD have been shown to be strong predictors of myelin content in postmortem human brain, the interpretation of changes in AD remain controversial since both increases and decreases have been reported [27].

It is clear that advances in MRI have been essential for a better understanding of the pathophysiology and clinical management of MS patients. Nevertheless, the improvement of advanced diffusion MR imaging techniques is still necessary

in order to gain a better understanding of the disease and to improve the value of MR imaging in MS clinical assessment, especially with respect to its potential prognostic value [28].

Chapter 3

Projected DTI indices as new measures to study WM integrity

3.1 Motivation and objectives

DTI indices have been used in several white matter studies in attempt to qualify and quantify structural changes in the tissues. However, in order to take meaningful and accurate conclusions from this type of studies it is necessary to consider the limitations of DTI technology.

DT-MRI data is analysed based on the assumption that the principal eigenvector of the DT is aligned with the direction of the white matter tracts. However, this supposition is not always valid, as in the case of voxels containing crossing fibres. Furthermore, besides this intrinsic limitation of the DT model, there are other issues that deviate the DT from the axonal bundles' genuine direction: a low SNR of the DW-images, and the presence of lesions. In these voxels, the terminology of axial and radial diffusivities becomes no longer adequate to represent, respectively, the molecular mobility along and across the WM tracts, because the DT eigenvectors are oriented along other biological structures. Not considering the geometrical features of the tensor ellipsoid can, in this way, result in misleading conclusions when comparing diffusion properties between group populations, especially, between healthy subjects and patients. In order to prevent deceptive interpretations of the tissue's biophysical changes, the alignment of the DT principal direction should be checked with the underlying tissue structure geometry.

This problem was explored by Wheeler-Kingshott et al. [1, 29], who suggested a novel methodology to quantify diffusion based on projected diffusivities [1]. Two new indices were introduced: the Projected Axial Diffusivity (PAD) and the Projected Radial Diffusivity (PRD). These parameters measure diffusion along reference directions derived from a DT-dataset representative of the healthy brain, thus

allowing a coherent comparison of diffusivity properties between subjects and independent of focal brain lesions. To test this approach, Wheeler-Kingshott et al. conducted a pilot study on two MS patients, using the projected parameters to look for differences between each patient and a group of controls. The results suggested that the projected indices can give more information about MS pathology than the standard ones when the clinical condition is more severe.

The aim of this work is to develop a pipeline for comparative studies of MS patients and controls' groups using this new approach and to test its feasibility for studying WM pathology. More specifically, this work will assess if the projected parameters, PAD and PRD, can depict different structural changes between controls and patients compared to their analogous standard parameters, AD and RD. In addition, differences in the orientation of DTs' between healthy subjects and MS patients will be studied with the purpose of investigating if there are major differences between the two groups due to MS pathology. Finally, the analysis' results will be related to the areas of WM lesions detected by conventional MRI.

3.2 Methods

The methodology of this study can be divided into six main stages:

- Processing pipeline;
- Registration;
- Calculation of DTI indices;
- DTI indices statistical analysis;
- Angle calculation and analysis;
- Creation of the Lesion Probability Map (LPM);

First, the DW-images were processed and used to calculate the DT-images. Subsequently, each DT-dataset was registered to a template created from a subset of healthy controls and MS patients.

Then, the standard anisotropic indices of diffusion, AD, RD and FA, and their correspondent projected parameters, PAD, PRD, Projected Fractional Anisotropy (PFA), were calculated. These measures were used to look for statistical significant differences between the group of controls and the group of MS patients. After that, the results of each pair of analogous parameters were compared.

In order to analyse the difference in the tensor's orientation between the DT-datasets of controls and patients, the DT-datasets of each group were averaged and then, for each voxel, the angle between the principal direction of each mean DT-dataset was calculated.

Finally, a lesion probability map was created from standard T2-weighted scans to relate the study results to the MS patients' areas of WM lesions that were detected by conventional MRI.

3.2.1 Data and processing pipeline

Subjects

The study population of this research was constituted by 124 subjects: 48 healthy controls and 76 MS patients. Twenty patients had a PP disease type, 27 were RR and 29 were SP. The demographics and clinical characteristics of the participants are described for the controls and for the different groups of patients in Table 3.1. The information regarding the clinical condition of the patients is given by the parameter Disease Duration (DD), which corresponds to the number of years that have passed since the patients were diagnosed; and by the EDSS score.

Table 3.1: Subject group descriptives (mean \pm standard deviation).

| Subject | Age (years) | Sex (M/F) | Median EDSS (range) | DD (years) |
|----------------|-----------------|-----------|---------------------|-----------------|
| HC | 41.7 \pm 13.0 | 24/24 | - | - |
| MS patients | 48.7 \pm 10.1 | 26/50 | 6 (1-8.5) | 15.9 \pm 10.0 |
| PP MS patients | 51.3 \pm 10.1 | 7/13 | 6 (1.5-6.5) | 12.9 \pm 7.72 |
| RR MS patients | 42.0 \pm 9.56 | 9/18 | 1.5 (1-6.5) | 10.8 \pm 8.62 |
| SP MS patients | 53.2 \pm 7.19 | 10/19 | 6.5 (4.5-8.5) | 22.8 \pm 8.69 |

Initial data

At the beginning of this project I was given a set of initial data for each subject, which is listed below:

- Eddy-corrected DW-data;
- Text files with unitary vectors representing the gradient directions and the corresponding b values of each acquisition;
- The transformations resultant from the eddy-current corrections.

Eddy currents are electric currents originated from the time-varying magnetic field that is formed during the DW-image acquisition. These currents generate residual magnetic field gradients that, in turn, combine with the applied imaging gradient pulses. Consequently, the gradients experienced by the spins are not exactly the ones established for the acquisition, which causes distortions in the reconstructed DW-image. To minimize the artefacts caused by the distortions, eddy correction

techniques are employed [30]. In this case, the DW-data was eddy-corrected using the FMRIB Software Library (FSL) (<http://fsl.fmrib.ox.ac.uk/>), which consists in a set of analysis tools for functional MRI, MRI and DTI brain imaging data.

For the patients, I was given further data in order to create the LPM:

- T2-weighted MRI scans;
- Region of Interest (ROI) lesions masks drawn in the T2-weighted scans by an experienced neurologist of the group.

MRI Protocol

The MRI scans of the brain were acquired using a Philips Achieva 3T system (Philips Healthcare, Best, The Netherlands) with a 32-channel head-coil.

The DW-data was acquired with a diffusion-weighted spin-echo echo-planar imaging (DW-SE-EPI) sequence. In addition, the following parameters were used: Echo Time (TE) = 68 msec, Repetition Time (TR) = 24 sec with cardiac gating to limit physiological noise artefacts, $2 \times 2 \times 2 \text{ mm}^3$ voxel size, 61 isotropically distributed diffusion-weighted directions with $b = 1200 \text{ s.mm}^{-2}$ plus 7 non diffusion-weighted ($b = 0$) (B_0) volumes.

The T2-weighted scans were acquired with a dual-echo sequence ($1 \times 1 \times 3 \text{ mm}^3$, TR = 3500 msec, TE = 19/85 msec).

DT estimation

For each voxel, the DW-data was used to reconstruct information about the diffusion orientation, fitting it to an ellipsoid. The DT estimation was done using the UCL Camino Diffusion MRI Toolkit (<http://cmic.cs.ucl.ac.uk/camino>), which is an open-source software toolkit for diffusion MRI processing.

Camino has a range of standard and advanced fitting algorithms. For this work, a linear diffusion tensor model was used, in which the elements of the diffusion tensor are calculated from a standard linear least-squares fit.

To perform the fitting, it was necessary to define a schemefile listing the details of the acquisition of each DW-image. This was made using the information about the gradient directions and the b-values. However, before doing this step, the gradient vectors needed to be rotated according to the eddy-current correction transformations. This rotation was applied using FSL.

After the fitting, the DTs' information was saved in a 5-dimensional image (dim1=112, dim2=112, dim3=72, dim4=1, dim5=6) with the first 3 dimensions representing the size (x,y,z) of the image, the 4th dimension indicating that there

is no time axis, and the 5th dimension representing the 6 components of the tensor: Dxx, Dyx, Dyy, Dzx, Dzy, Dzz.

3.2.2 Registration

This work uses a Voxel-Based Analysis (VBA) to anatomically localize WM differences between the groups of controls and patients. Before conducting a VBA it is mandatory to spatially normalize all DT-images in order to remove the size and shape differences of the brains. After spatial normalization, correspondent voxels across the cohort should represent the same anatomical structures and any remaining differences between subjects should correspond to differences in their diffusion properties.

Choice of the registration method

Different methods for normalizing DT images have been proposed in the literature. In the most simple procedures, the registration is performed using DTI scalar indices, such as FA, so that it is possible to use the traditional intensity-based registration methods [31]. However, this scalar-based normalization method doesn't consider the orientation information encoded in the DTs, which is of major importance since each DT should be aligned according to the image's underlying anatomical structure [7]. In order to maintain the DTs orientation consistent with the subject anatomy after image transformation, it is necessary to reorient the tensor fields according to the performed transformation. The importance of this procedure is illustrated in Figure 3.1.

One of the reorientation strategies commonly used to reorient the DT images is the Preservation of Principal Directions (PPD) algorithm [32]. It rotates the DT in a way consistent with the reorientation of the tissue caused by the registration. On the other hand, the size and shape of the tensor, i.e. its eigenvalues, are preserved, because they reflect the properties of the underlying tissue microstructure [32].

More complex registration methods use full tensor information. DTI-TK (<http://dti-tk.sourceforge.net>) [34, 35] is a publicly available tool that performs spatial normalisation of DTI data. This registration algorithm matches tensors as a whole, which improves the alignment of diffusion tensor images compared to the scalar-based method.

Due to the enhanced performance in tensors alignment compared to other spatial normalization methods [36], DTI-TK was chosen to perform the registration in this work. Thus, using this toolkit, each DT-dataset was registered to a DT-image template.

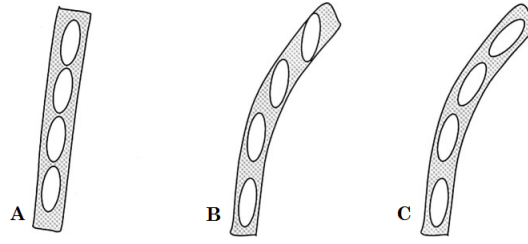


Figure 3.1: Importance of tensor reorientation after registration. A - In the original DT-image, the tensor field is aligned with the axonal fibre. B - After being warped with the scalar-based registration transformation, the tensors are no longer aligned with the underlying anatomy. C - However, reorienting the tensors after the scalar-based registration, realigns the ellipsoids with the fibre track. Image adapted from [33].

Preprocessing

Before using DTI-TK, it was required to perform a preprocessing step on the DT-data.

First, the non-brain tissues were removed from the images using the Brain Extraction Tool (BET) [37] of FSL, which is an automated method for separating the brain tissue from the non-brain tissue of MR head images.

This tool couldn't be applied directly to the DT-datasets nor to the DW-images, due to their contrast. Instead, the 7 B0 images of each participant were averaged and then the resulting mean image was used with the BET tool. This tool has an option to choose a fractional intensity threshold that determines the edge of the brain outline. It ranges from 0 to 1 and its default value is 0.5. For this dataset, a value of 0.2 was chosen, which results in a larger estimated brain than the default. This value was chosen because it was the best at avoiding the removal of brain tissue and at minimizing the quantity of non-brain tissue kept. Finally, each DT-dataset was masked with its correspondent brain-extracted mean B0-image.

The next step was to ensure that the DT-datasets were SPD matrices. Although this condition is part of the definition of a tensor, in practice, during the DT estimation, the noise from the DW-images may cause this not to happen in some voxels. This usually occurs in the voxels around the boundary of the brain, due to an imperfect brain extraction, and in the voxels where there was an imperfect correction of motion or eddy-current distortions. Nonetheless, this condition is important to make sure that the DT-datasets behave correctly after successive processing steps. Using a tool in DTI-TK, it was possible to identify the non-SPD voxels and enforce this condition on them. In addition, by observing the images of the non-SPD voxels, it was possible to check that this condition was verified in very few voxels inside the brain, revealing that the DW-data was not markedly noisy.

Template

Using a population-specific template, that is morphologically closer to the subjects in the cohort, can improve the accuracy of registration. Therefore, the template was created using a subset of the study population, constituted by 20 healthy controls and 20 MS patients.

The template was constructed from both patients and controls in order to minimize the transformations needed in the registration for each subject. If the template was based on a healthy population alone, it would imply stretching the MS brains to a larger degree than healthy brains when performing registration.

The subjects for the template were chosen so that the average characteristics (age, sex and EDSS) of the subset were representative of the entire cohort. The information regarding the MS course of the disease for each patient was only available after the registration phase of the project. For this reason, the MS type is not as equally distributed between the patients' group as it would have been desirable.

A higher number of participants from the cohort was not included in the template because it would have demanded a longer computation time and this number of subjects was considered to be sufficient to create a representative template of the study population.

The characteristics of the individuals chosen for the template are shown in Table 3.2.

Table 3.2: Template group descriptives (mean \pm standard deviation)

| | HC | MS Patients |
|-----------------------|-----------------|-----------------|
| Age(years) | 51.3 \pm 10.1 | 46.9 \pm 13.0 |
| Sex(M/F) | 7/13 | 11/9 |
| Median EDSS (range) | - | 4.25 (1-8.5) |
| DD(years) | - | 14.2 \pm 11.2 |
| Type of MS (PP/RR/SP) | - | (3/9/8) |

The template was built using DTI-TK [38], which has a pipeline specifically designed for constructing templates with DT-images. DTI-TK starts by bootstrapping an initial template and then optimizes it with affine and deformable alignments. The affine alignment uses linear transformations (rotation, translation, scale and shear) to change objects' global size and shape whereas deformable alignment removes size or shape differences between local structures using affine and non-linear transformations.

First, the selected DT-images were rigidly aligned to an existing template, recommended for the DTI-TK's spatial normalization pipeline, named "IXI aging tem-

plate” [39]. Since the rigid alignment includes only rotational and translational transformations, the IXI aging template doesn’t have any influence on the size and shape of the constructed template. The purpose of this step is just to locate and orient the final template in space in a consistent way with the standard template spaces, such as the Montreal Neurological Institute (MNI) brain space.

After the rigid alignment, the initial template is computed as a log-Euclidean mean of the registered DT-images. Log-Euclidean operations are used instead of usual Euclidean operations, because the latter are problematic when working on tensors. However, these difficulties are avoided when tensors are transformed into their matrix logarithms [40].

In the next steps, the averaged template is iteratively improved. The DT-images are registered to the template and then a refined template is obtained as the average of the registered DT images for the next iteration. This procedure is repeated until the difference between templates from consecutive iterations becomes sufficiently small, first with affine and then with non-linear registrations [41].

The final template can be observed in Figure 3.2.

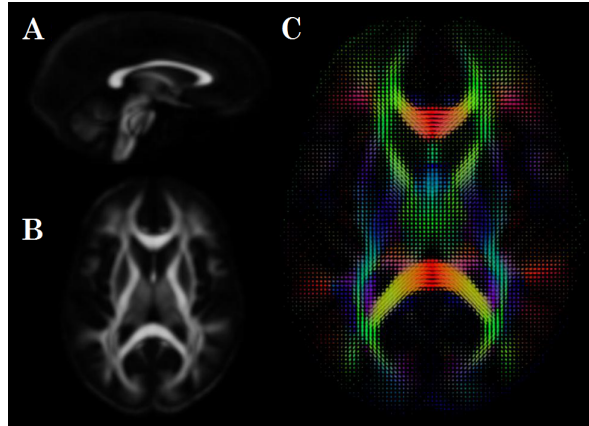


Figure 3.2: Template created. **A** - FA map (sagittal view). **B** – FA map (axial view). **C** - Ellipsoid representation with colour coding. Red corresponds to diffusion along the transverse axis; blue, to diffusion along the inferior-superior axis; and green, to diffusion along the anterior-posterior axis. The tensors in the genu and splenium (in red) of the corpus callosum should be aligned with the transverse axis, like in this image. This is a very important feature and allows checking if the tensors are correctly reconstructed.

Registration and image mapping

All the subjects were registered to the template using a pipeline involving rigid, affine and deformable alignment. For each subject, DTI-TK outputs two transformations (affine and deformable) that together define the mapping from the subject native space to the template space.

In order to minimize the smoothing effect of interpolation, it is desirable to warp the subject data to the template space with a single interpolation. Thus, it was necessary to use a DTI-TK command to combine the two transformations into one before applying it.

At the end of this stage, all DT-images shared a common space, allowing a voxel-based comparison between subjects.

3.2.3 Calculation of the DTI indices

Original indices

The eigenvectors and eigenvalues of each DT-dataset were extracted with DTI-TK and then, the maps for AD, RD and FA were calculated using their standard expressions with Matlab (<http://www.mathworks.com/>).

Projected indices

The projected parameters PAD, PRD and PFA were calculated by projecting the obtained tensors in the most likely healthy direction of diffusion. In order to define this healthy direction, the DT-datasets from the entire cohort of 48 controls were averaged in a DT-dataset of reference. Again, this was done using DTI-TK, which employs log-Euclidean metrics.

Then, for each voxel, the reference eigenvectors and their corresponding eigenvalues were extracted from the DT-dataset of reference. The projected indices were calculated according to their usual expressions but using the projected eigenvalues instead of the original ones obtained directly from the DT. In this work, the wording "projected eigenvalue" refers to the magnitude of the projection of all components of a DT in the direction of a certain reference eigenvector.

For each voxel of each subject n (with $n = 1, \dots, 124$), the j^{th} projected eigenvalue $\lambda_{n,j,proj}$ (with $j = 1, 2$ or 3) was calculated with Matlab according to the following expression:

$$\lambda_{n,j,proj} = (v_{j,ref})^T \cdot DT_n \cdot (v_{j,ref}) \quad (3.1)$$

Where $v_{j,ref}$ corresponds to the j^{th} reference eigenvector and DT_n corresponds to the diffusion tensor of that subject's voxel.

A description of the projected indices calculation process is summarized in Figure 3.3.

It is important to remark that, by definition, $\lambda_{1,proj}$ is never higher than the corresponding λ_1 , and that $\lambda_{2,proj}$ and $\lambda_{3,proj}$ are never smaller than λ_2 and λ_3 , respectively. Consequently, whilst PAD is never higher than the corresponding AD, PRD is never smaller than the corresponding RD.

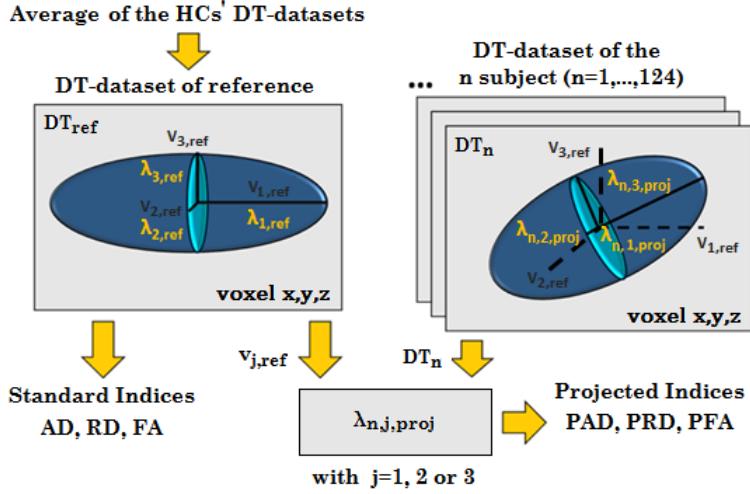


Figure 3.3: Schematics of the projected indices calculation.

In the previous published work with projected indices [1], the index PFA hadn't been considered. This parameter was included in this study because PFA informs about the anisotropy of the projected DT, which can be representative of changes in the alignment of the tensors.

3.2.4 DTI indices statistical analysis

The correspondent indices from controls and patients were statistically compared in order to identify the white matter areas with pathological abnormalities.

This analysis was conducted using the Statistical Parametrical Mapping (SPM) 8 software (<http://www.fil.ion.ucl.ac.uk/spm/software/spm8/>), which is used to identify regionally specific differences in the brain.

With this software, a VBA was performed to compare the indices AD, RD, FA, PAD, PRD, and PFA between controls and patients.

For each measure, the group of controls was compared with 6 different group combinations of MS patients:

- all 76 MS patients;
- patients with PP MS;
- patients with SP MS;
- patients with RR MS;
- SP and RR patients with EDSS<6;
- SP and RR patients with EDSS≥6.

For each analysis, a 2-sample t-test was used, with age and sex as covariates. In addition, to ensure that only the white matter was considered in the study, an

analysis mask was defined from the FA map of the template thresholded for voxels with $FA \geq 0.3$.

The differences between patients and controls were deemed to be significant for a $p\text{-value} < 0.05$, after correcting for the Familywise Error Rate (FWE) for multiple comparisons.

Before performing the statistical analysis, the images were smoothed with SPM8 [42] by being processed with a low pass filter derived from a Gaussian kernel with Full Width at Half Maximum (FWHM) of 8-mm. This step is very important for increasing the validity of the results: it makes the data more normally distributed, which is a property required by SPM; it improves the SNR; and it helps attenuating imperfections from the registration.

The width of the smoothing kernel was chosen based on the recommendations of a study that investigated the best filter size in DT-MRI data analysis [17] and by observing the results obtained with different filter sizes.

The output of each analysis is a statistical map showing regions where the brain differs significantly among the two groups.

3.2.5 Angles calculation and analysis

It was studied how the orientation of the tensors differed between the average of controls and the average of patients.

First, identically to the process of averaging the controls' DT images, which resulted in the DT-dataset of reference, the mean of the MS patients' DT-images was calculated.

Then, for each voxel, the angle separating the corresponding tensors of each mean DT-dataset was calculated using the definition of the dot product:

$$\alpha = \text{Arccos} \left(\left| \frac{v_{1,ref} \bullet v_{1,ms}}{|v_{1,ref}| |v_{1,ms}|} \right| \right) \quad (3.2)$$

Where $v_{1,ref}$ and $v_{1,ms}$ correspond, respectively, to the principal eigenvector of the reference DT-dataset and to the principal eigenvector of the MS patients' mean DT-dataset.

The angle α was calculated from the absolute value of the dot product because, although the two principal eigenvectors may form an angle greater than 90° , the smaller angle between the two tensor principal axes never goes beyond that value.

Finally, the resulting volume was thresholded for voxels with $FA \geq 0.3$ and then the magnitudes of the angles were observed to investigate the areas with higher dispersion between the two averaged groups.

3.2.6 Creation of the lesion probability map

To relate significant differences between patients and controls with the localization and extension of the lesions detected with standard MRI, it was necessary to create a LPM. This map represents the likelihood of finding a lesion in a certain voxel across a group of patients.

As previously mentioned, the LPM was created from T2 hyperintense MS lesion masks drawn by an experienced neurologist.

First, the lesion masks, originally in their individual space, needed to be mapped into the common space of the DT-template. However, since it is not possible to register the T2 images to the information in a tensor image, the B0 images were used as target instead.

Therefore, a mean B0 template was created. The mean B0 image of each patient was mapped onto the DT template space by applying the correspondent transformation resultant from the initial DT-dataset registration. This was possible because for each subject, the original B0 scans and DT-datasets were in the same native space.

Subsequently, the B0 mean images in the template space were averaged, constituting a mean B0 template. Then, each T2-weighted MRI scan was registered to the B0 mean template using linear and non linear transformations from Nifty Reg (<http://sourceforge.net/projects/niftyreg/>). These transformations were combined into one single transformation, which was then applied to the lesion mask of the corresponding patient.

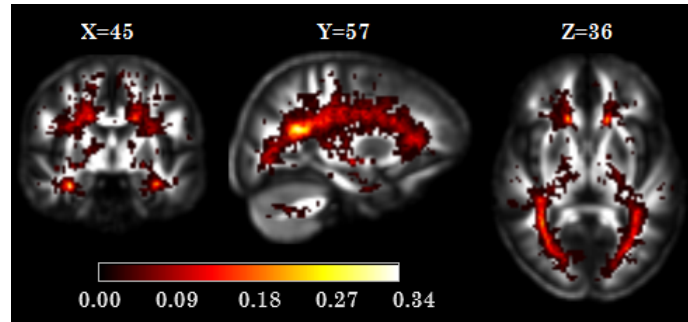


Figure 3.4: Lesion probability map created.

All registered lesion masks were binarized and then averaged. The resultant image is the final LPM, which is presented in Figure 3.4.

It can be observed that the cohort of patients had their lesions quite dispersed in the WM. In fact, the mean value of the LPM is 0.04, which correspond to the overlap of lesions in just 4% of the patients.

When relating the analysis' results with the presence of lesions, the LPM was

thresholded for values above 10%. Due to the dispersion of the lesions, it wouldn't be advantageous to threshold the map at a higher value. Thereby, the thresholded LPM show regions where at least 10% of the patients present lesions.

3.3 Results

3.3.1 Statistical analysis

Comparison between patients and controls

In comparison with the normal controls, all groups of MS patients presented regions with significantly increased AD, PAD, RD and PRD and decreased FA and PFA. No significant differences were found for the opposite case (decrease of AD, PAD, RD and PRD and increase of FA and PFA).

The extension of the differences obtained between the controls and the various groups of MS greatly differed between them. Regarding the MS types groups (PP, SP and RR), the highest extent of significant patient-controls differences was observed for the SP and $EDSS \geq 6$ cohorts and the smallest for the PP group.

Additionally, it was observed that, for each measure, the results of the analysis between the controls and the whole group of MS patients were very similar to the ones obtained between the controls and the SP group and between the controls and the $EDSS \geq 6$ group. This is understandable since the median EDSS of the 76 patients group is 6 and the median EDSS of the SP group is 6.5.

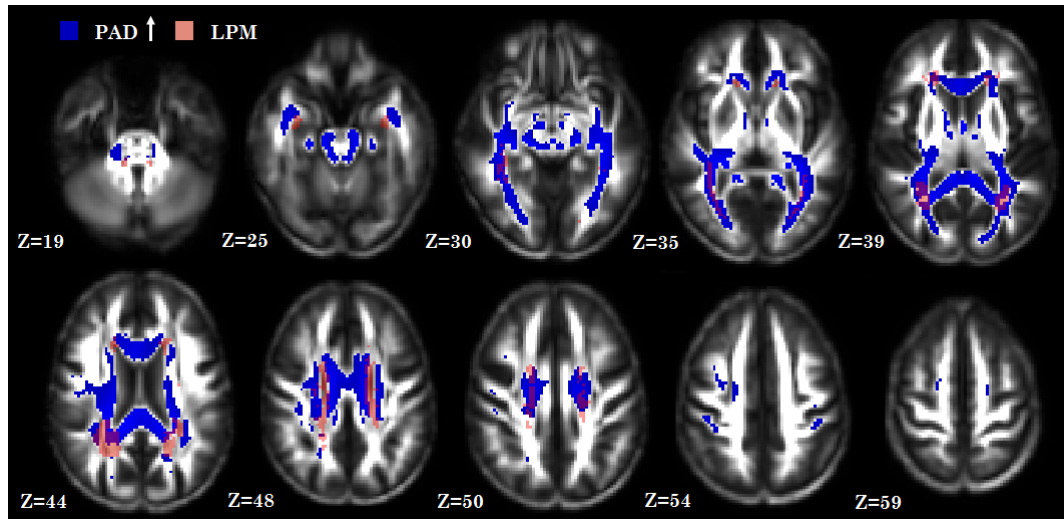


Figure 3.5: Results showing areas with increased PAD (blue) in MS patients comparing to controls. Pink represents the LPM thresholded at 10%.

The results obtained for an increase in PAD and PRD and a decrease in PFA, between the controls and the entire group of patients, can be found, respectively, in Figures 3.5, 3.6 and 3.7.

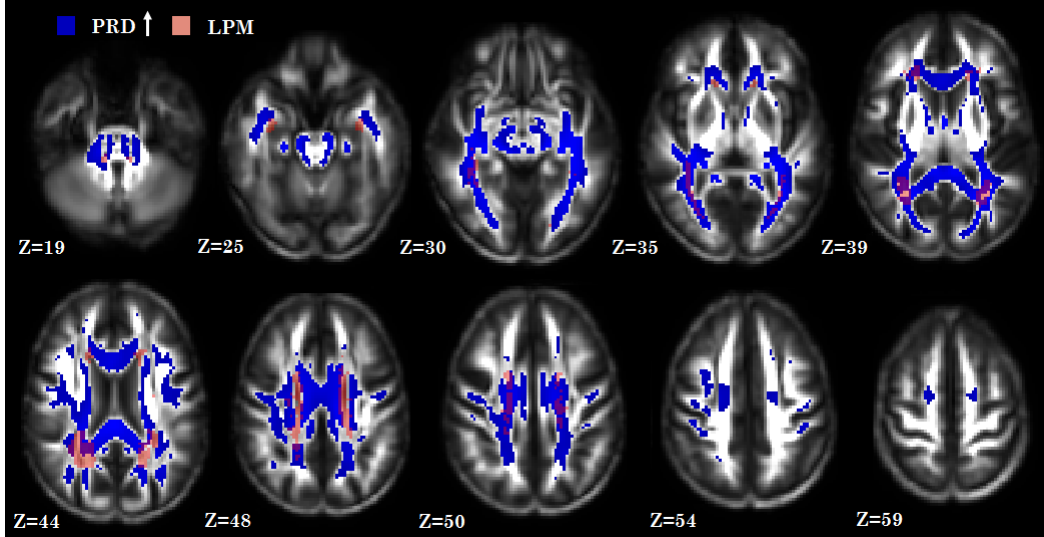


Figure 3.6: Results showing areas with increased PRD (blue) in MS patients comparing to controls. Pink represents the LPM thresholded at 10%.

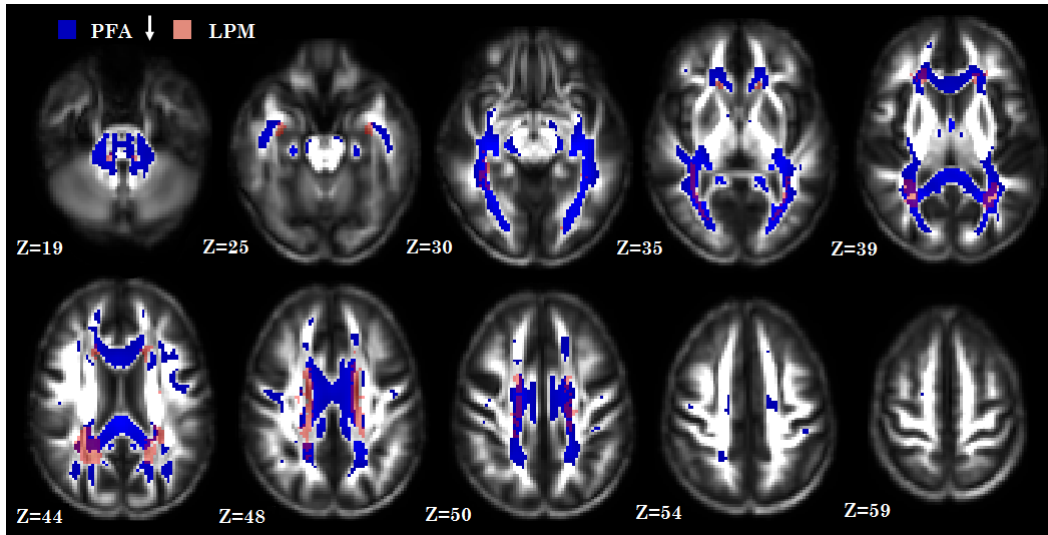


Figure 3.7: Results showing areas with decreased PFA (blue) in MS patients comparing to controls. Pink represents the LPM thresholded at 10%.

In general, the increase of RD and PRD was found in more areas than the changes in the rest of the measures. Nonetheless, there are a lot of regions where the changes between the indices PRD, PAD and PFA (Figures 3.5-3.7) and between the indices AD, RD and FA overlap with each other.

Additionally, it was common to find regions where areas of indices' changes overlapped with the LPM thresholded at 10%. These changes usually extended to regions outside the lesions. However, there were also regions where the thresholded LPM was not accompanied by significant changes in the parameters.

Original and projected indices

The purpose of this analysis was to investigate whether the projected indices (PAD, PRD and PFA) would present higher sensitivity to white matter changes caused by MS pathology than the standard indices (AD, RD and FA).

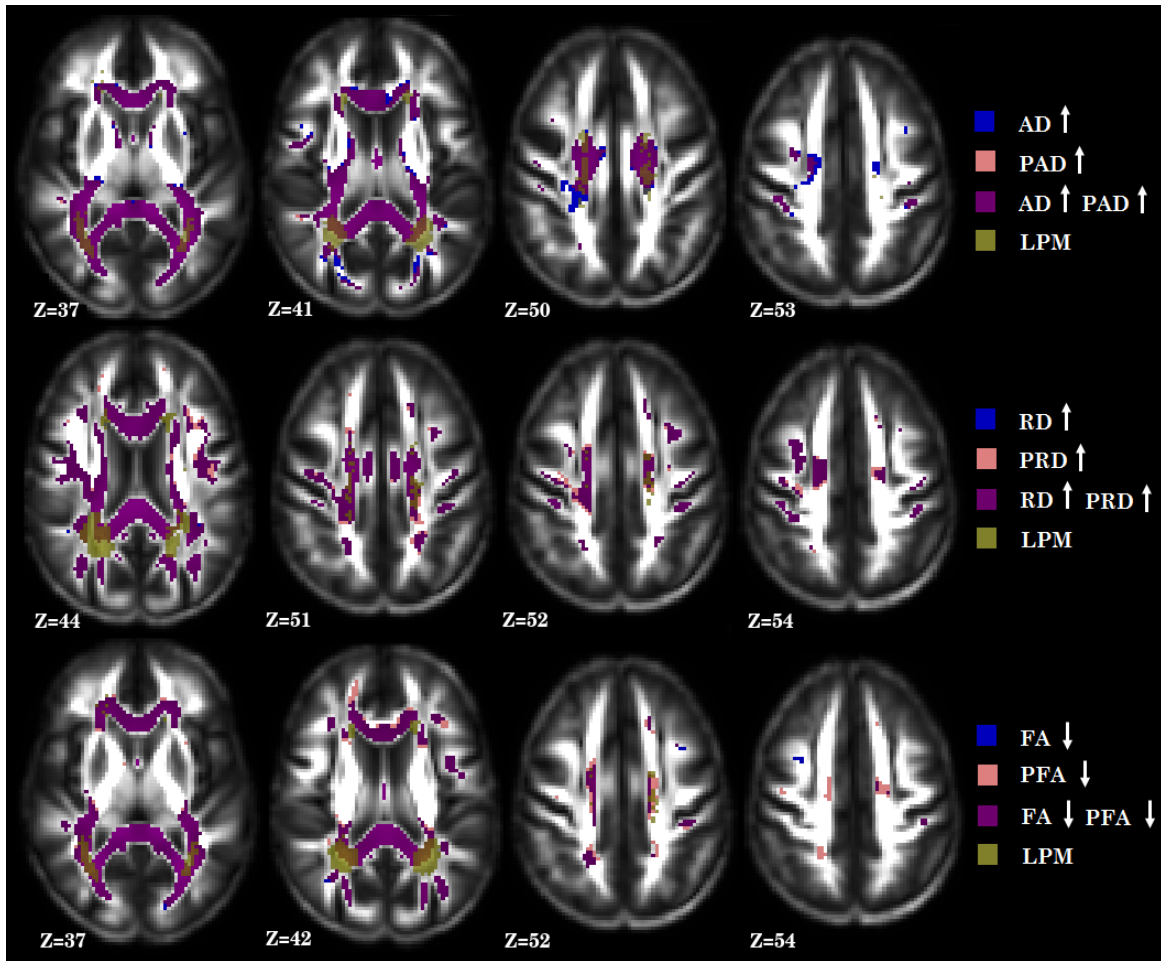


Figure 3.8: Comparison between the projected and original indices, considering all MS patients. Blue and pink represent areas with changes in the MS patients detected, respectively, with the standard and the projected parameters. In addition, purple corresponds to the overlay between the blue and the pink areas and the olive green represents the LPM thresholded at 10%.

The results showed that changes detected with the projected parameters mostly overlapped with the ones detected with the standard parameters, with exception to

some voxels or small areas (Figure 3.8).

This observation was common to the results between the controls and all the different MS groups. For this reason, the only differences between the projected and original indices that are reported in this work belong to the analysis between the two entire cohorts.

In general, the areas with increase of PAD were less extensive than the areas with increased AD. Conversely, the areas with increase of PRD and decrease of PFA were more extensive than the areas with increase of RD and decrease of FA, respectively. Nonetheless, the maps of changes in RD and PRD were the ones showing less differences between the two.

Differences between the projected and original parameters were more frequently found in the superior part of the brain. In addition, some small regions where a decrease in PFA occurred as a result of an increase in PRD were observed. However, the analogous didn't happen regarding changes in the standard parameters (Figure 3.8 slices 52 and 54).

Since the changes in the two types of parameters were very similar, it is difficult to relate their differences with the thresholded LPM. Nonetheless, in Figure 3.8, in slices 50 and 53 from the first row, there are some voxels where an increase of AD coincides with the thresholded LPM or is in the surrounding area and there are no significant changes in PAD. On the other hand, in slice 52 from the second row and in slice 52 from the third row, the thresholded LPM seems to extend from the original measures RD and FA to the projected PRD and PFA, respectively.

3.3.2 Angles analysis

In this analysis, the angle between corresponding DTs of controls and patients' averages was measured for the WM.

Most voxels from the angle map showed very small differences between the orientation of corresponding mean DTs (Figure 3.9). The deviation between the two varied mostly between 0 and 5 degrees, although, in some voxels or in certain small areas, this difference increased. In fact, there were some well defined regions where the angles varied from 10 to 20 degrees.

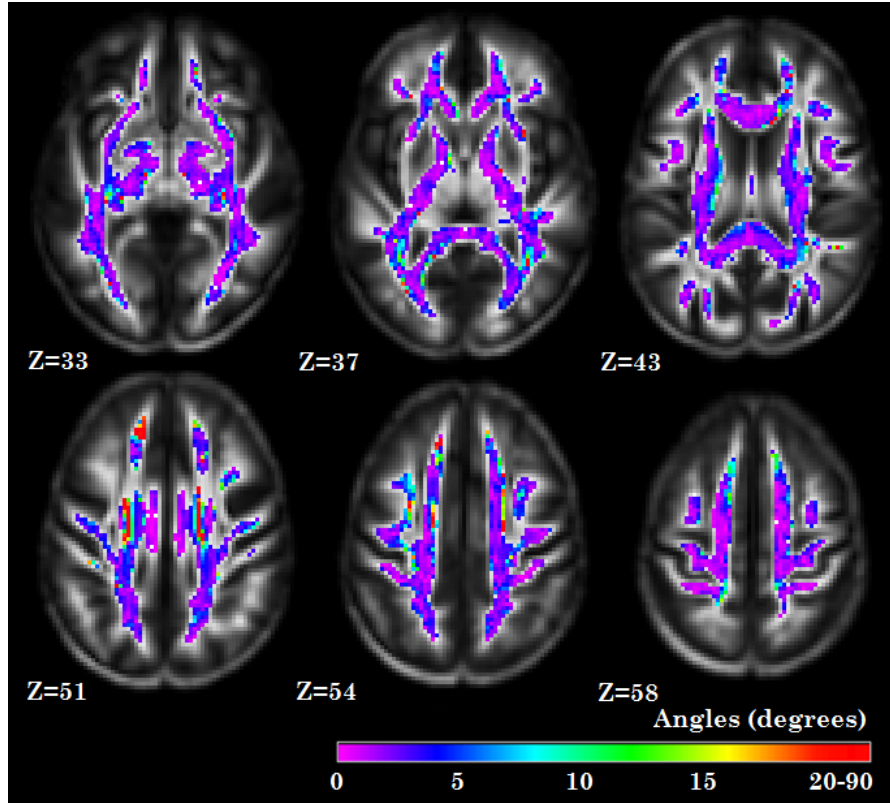


Figure 3.9: Results of the angle dispersion analysis between the mean DT-datasets: values of the angles between the corresponding tensors of the mean MS patients DT-dataset and the mean HCs DT-dataset.

3.4 Discussion

In this work, brain white matter changes in MS were investigated by standard diffusion indices (AD, RD and FA) and by projected diffusion indices (PAD, PRD and PFA) with the purpose of validating the latter as a more consistent approach to study white matter integrity in diseased brains.

The analysis started by comparing the HCs with different MS groups in order to assess if the differences between the standard and projected measures would vary according with the clinical characteristics of the patients. However, the differences in the patients-controls changes detected by the projected and by standard parameters were similar for all the different comparisons: the changes detected by the two different approaches mostly overlapped. Therefore, this study focused only on analysing the results between the statistical comparison of controls and the entire cohort of patients.

The WM abnormalities detected with the standard and projected indices were compared, so that it was possible to conclude whether this new approach could

give a more consistent means to study the WM damage caused by MS. Compared with the HCs, the patients exhibited reduced FA and PFA and increased AD, PAD, RD and PRD. In addition, for the two approaches, differences between patients and controls were frequently found in regions overlapping or surrounding the LPM thresholded at 10%.

However, at a group level there were no major differences between the standard and the projected indices. The MS changes detected by the analogous indices generally overlapped, differing only in some small regions. An increase in AD occurred in more areas than an increase in PAD and changes in PRD and PFA were extended over a greater number of voxels than changes in RD and FA, respectively.

This might be justified by the intrinsic properties of the projected indices. For every subject, in the voxels where the DTs are deviated from the principal eigenvector of the DT-dataset of reference, PAD is going to be smaller than AD, PRD is going to be greater than RD, and, consequently, PFA is going to be smaller than FA. Therefore, in a certain voxel, if the tensors are more deviated from the reference DT-dataset in the MS patients than in the controls, the increase in AD in the patients is going to be higher than the increase in PAD, which may not reach the significance level. On the other hand, the changes in PRD and PFA are going to be greater than the changes in RD and FA, respectively.

In fact, the small differences observed between these two types of parameters suggest that the projected measures PRD and PFA may have an increased sensitivity for detecting WM pathology. Specifically, there are regions where changes in PFA overlap with changes in PRD and RD while there are no changes in FA. Perhaps the changes in PAD would have been more extensive than AD changes if it was possible to identify significant decreases in these parameters. However, PAD may still be reflecting a more biologically sound quantity. The effect of noise in DW-images can cause an overestimation of the principal eigenvalues during DT fitting [43], leading to a fictitious increase in AD.

Due to the similarity in the number and extent of standard/projected indices changes when comparing the controls with the different groups of MS, there was no suggestion that the course of the disease or an increase in the severity of pathology could increase the number of differences between the two types of indices. However, in general, further information given by the projected parameters at an individual level might have been averaged out at a group level.

An important possible source of bias in the methodology of this work should be considered. The construction of a DT-dataset of reference obtained by averaging the cohort of controls, aimed to define, for each voxel, the most probable direction of diffusion in the healthy WM fibres. However, the individual normal variability in

the WM tracts may present an obstacle to this definition. For example, it is known that age affects the DT properties. Due to these considerations, Wheeler-Kingshott et al. [29] suggested that when using this approach the DT-dataset of reference should be built particularly for each study, in order to match the controls' population descriptives with the age and gender of the cohort under study. However, this may still not be enough to overcome the variability issue. For this reason, it is important to analyse the coherence of the tensors between the cohorts.

In this work, the angle between corresponding tensors of the mean DT-dataset of controls and the mean DT-dataset of patients was calculated. The results showed that in the WM, in general, there was a small (0 to 5 degrees) deviation between the tensor average of the two groups. This small difference, that is within the "cone of uncertainty" associated with the estimation of DTs principal direction [44], should be due to the fact that individual pathological deviations of MS tensors from the healthy fibre direction are cancelled during the cohorts average. However, there are some areas where this angular dispersion reaches up to 20 degrees. Although some of these voxels overlap or surround the thresholded LPM areas, the resultant deviation may not be due to pathology but to areas of crossing fibres.

In order to conduct a deeper analysis on this matter, it would be important to analyse the spatial dispersion of correspondent tensors across the HCs cohort. It would also be important to assess how the DT-dataset of reference would vary according to the healthy population chosen to be averaged. These two analyses could elucidate whether it is suitable to estimate the most likely direction of the WM tracks by this methodology.

Nevertheless, to make a final conclusion regarding the feasibility of the projected approach, it is desirable to investigate the pathological substrate of the projected measures with post-mortem studies.

3.5 Conclusion

In this study, a new pipeline for studying white matter pathology with DTI was developed and tested. Projected DTI indices (PAD, PRD and PFA) were calculated from the projection of the DTs along reference directions provided by the eigenvectors of a DT-dataset representative of the healthy population. This approach was presented as a more biologically meaningful way of comparing DTI quantities between subjects, especially between controls and patients.

To summarize, it was shown that, despite only minor differences in the patients/controls changes detected with the standard and projected methodologies, there were some indicators of higher sensitivity in the latter. Nevertheless, it is

not possible to make a final consideration regarding the sensitivity of the projected parameters based solely on the results of this work. Further studies are necessary to investigate the biological substrate of the projected approach.

Chapter 4

The effect of registration on VBA of DT-MRI data

4.1 Motivation and objectives

The registration technique employed for registering the DT-images is very important for the purpose of this research, since the projected indices are calculated according to the tensors' orientation.

In the first part of this project (Chapter 3), DTI-TK was chosen to spatially normalize the DT-datasets for having a better performance than other methods at aligning the DTs with each other [36]. However, although this is valuable when considering healthy subjects, it might not be advantageous when investigating controls-patients changes, because the DT-based registration may cancel the orientational pathology-derived differences by forcing the DT eigenvectors to be aligned with the template. In fact, with this methodology, the results showed small variations in the patient-controls changes detected with the original and with the projected parameters.

Furthermore, in the article introducing the projected diffusivities, the authors performed a scalar-based registration, where the FA map of each subject was registered to the FA map of the template. This study showed that at an individual level and in patients with severe clinical MS, the projected approach would give different and possibly new information regarding MS pathology compared to the standard one [29].

With the purpose of investigating whether the results from the previous analysis (Chapter 3) could be biased by the registration technique employed, the group analysis was performed a second time. In the present study, the normalization pipeline used was based on realigning FA rather than the DT itself. In addition, this study also assessed the importance of the registration methodology when investigating

differences in DT-derived indices between patients and healthy subjects.

4.2 Methods

The DT-MRI data was registered with a FA-based method. The target template was kept the same as for the previous analysis, with the difference that the FA map corresponding to the template was calculated using DTI-TK and used as the target reference for the single subject registration.

First, the FA map of each DT-dataset was calculated in its individual native space (with DTI-TK) and then, using NiftiReg, the FA maps were registered to the FA template with affine and non-linear transformations. For each subject, these two transformations were combined into one and then the resulting transformation was applied to the corresponding DT-dataset in its individual space. The spatial transformations were applied using a DTI-TK command that includes the PPD algorithm. Therefore, the tensors were warped without losing their orientational information.

After registration, similar procedures to the ones explained in the previous study were used for the data analysis. First, the changes in the original and projected parameters were assessed between the group of controls and the whole group of patients: the projected eigenvalues were calculated using the Eq. 3.1 and the same DT-dataset of reference constructed with DTI-TK; the DTI indices AD, RD, FA, PAD, PRD and PFA were calculated for each subject using the same previous expressions; and then, the same methodology was employed for the statistical analysis, which compared correspondent indices from controls and patients on a group basis.

Similarly to what was done before, the tensors' orientation between the average of controls and patients was analysed: the HCs and MS patients' DT-datasets were averaged using DTI-TK; and then, the angles between the corresponding tensors of the two DT-datasets were calculated.

In addition, the dispersion of tensors' orientation was also investigated between the two mean HCs datasets obtained with the two different registration pipelines.

Finally, the results were assessed. The MS changes in the original and projected parameters obtained in this study were compared with each other, and the MS changes in the original parameters obtained with the FA-based registration were compared with the original parameters obtained with DTI-TK registration. The calculated angle maps were visually analysed. In addition, a normalized histogram of the magnitude of the angles maps (angles between controls and patients using the DT-based and the FA-based pipelines, and angles between the controls obtained with the two registration pipelines) was obtained. Then, the percentage of WM

voxels with angles above 5 degrees was obtained by calculating the area below each histogram correspondent to this angular difference. This was done to compare the role of registration in the overall alignment of the tensors. The LPM used to analyse the results was the one obtained in the DT-based registration analysis (Chapter 3).

4.3 Results

4.3.1 Statistical analysis

Once again, significant differences were found only for an increase of AD, PAD, RD and PRD and for an decrease in FA and PFA in patients comparing to controls.

Changes detected with FA-based versus DT-based registration

The changes in the standard parameters obtained using the DT-based and the FA-based pipelines were compared (Figure 4.1). The results from both methods usually overlapped, however, in some regions, changes were only detected with the DT-based pipeline or only with the FA-based pipeline.

For example, there were considerably large regions where the increase in AD was exclusively detected with the DT-based registration (Figure 4.1, first row). In addition, in Figure 4.1 there are areas with a decrease in FA (third row, slice 39) only detected by the DT-based pipeline. In general, the changes detected exclusively with the FA-based registration were also frequent but had a smaller area and were mainly distributed in the superior part of the brain (Figure 4.1, third row). Finally, the patients-controls differences in the RD parameters also varied according to the registration pipeline used, but to a less extent (Figure 4.1, second row).

The thresholded LPM mostly overlapped with changes that were detected with both pipelines. However, in Figure 4.1, first row, slice 50, the LPM overlaps with changes exclusively detected by the DT-based AD.

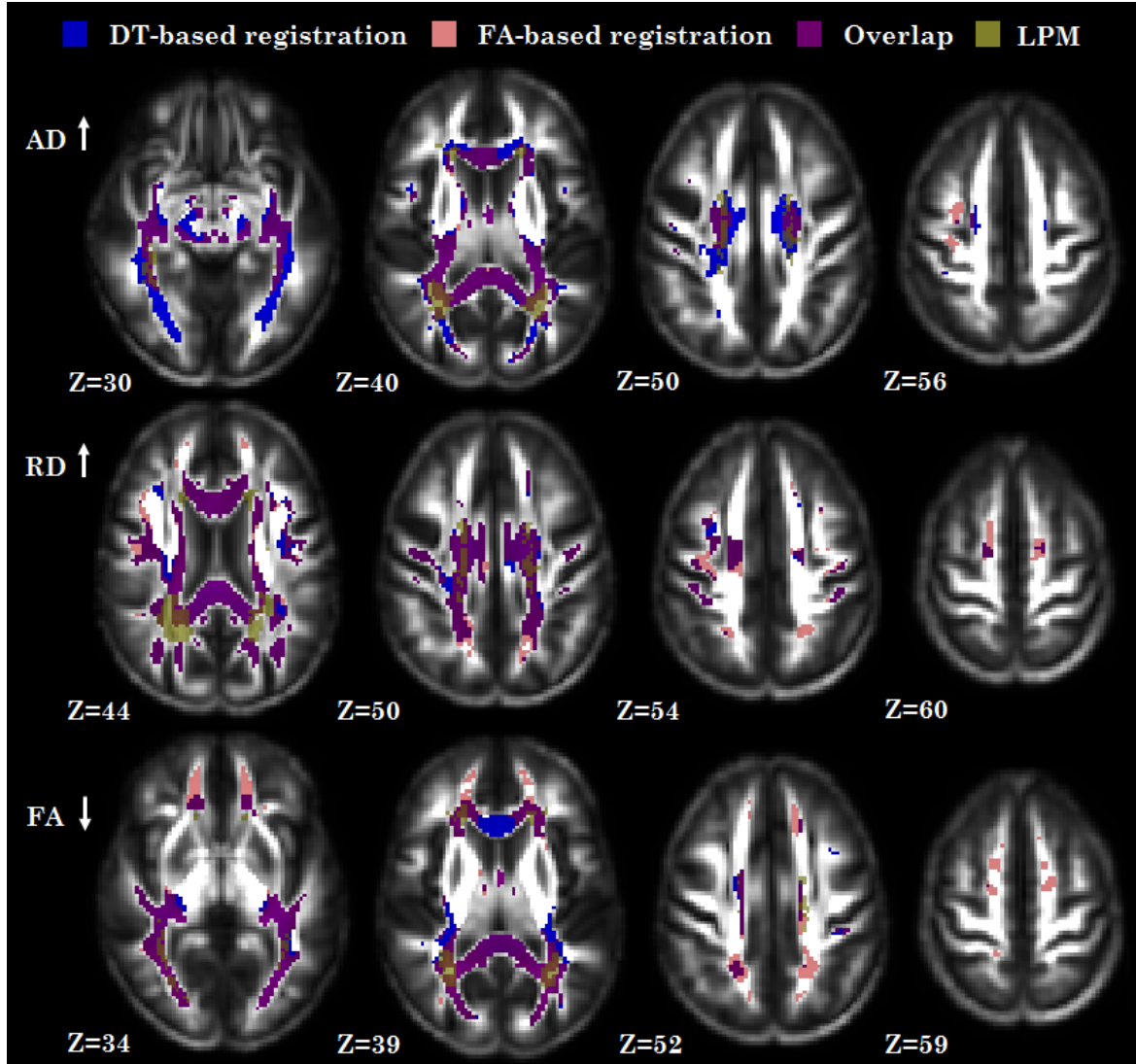


Figure 4.1: Results of the comparison between the changes (patients versus controls) in the original parameters obtained with FA-based registration (pink) and with DT-based registration (blue). The overlay between the two is represented in purple and the olive green corresponds to the LPM thresholded at 10%.

Original and projected indices detected with FA-based registration

The original (AD, RD and FA) and the projected indices (PAD, PRD and PFA) obtained with the FA-based pipeline were compared between the HC and the MS patients. The changes identified by each pair of measures were compared and related with the LPM (Figure 4.2).

Similarly to the previous analysis (Chapter 3), the WM changes in the analogous projected and original parameters mostly overlapped. Areas of increased PAD in MS patients compared to HC were more localized than areas of increased AD, which extended over a greater number of voxels. On the other hand, an increase in PRD

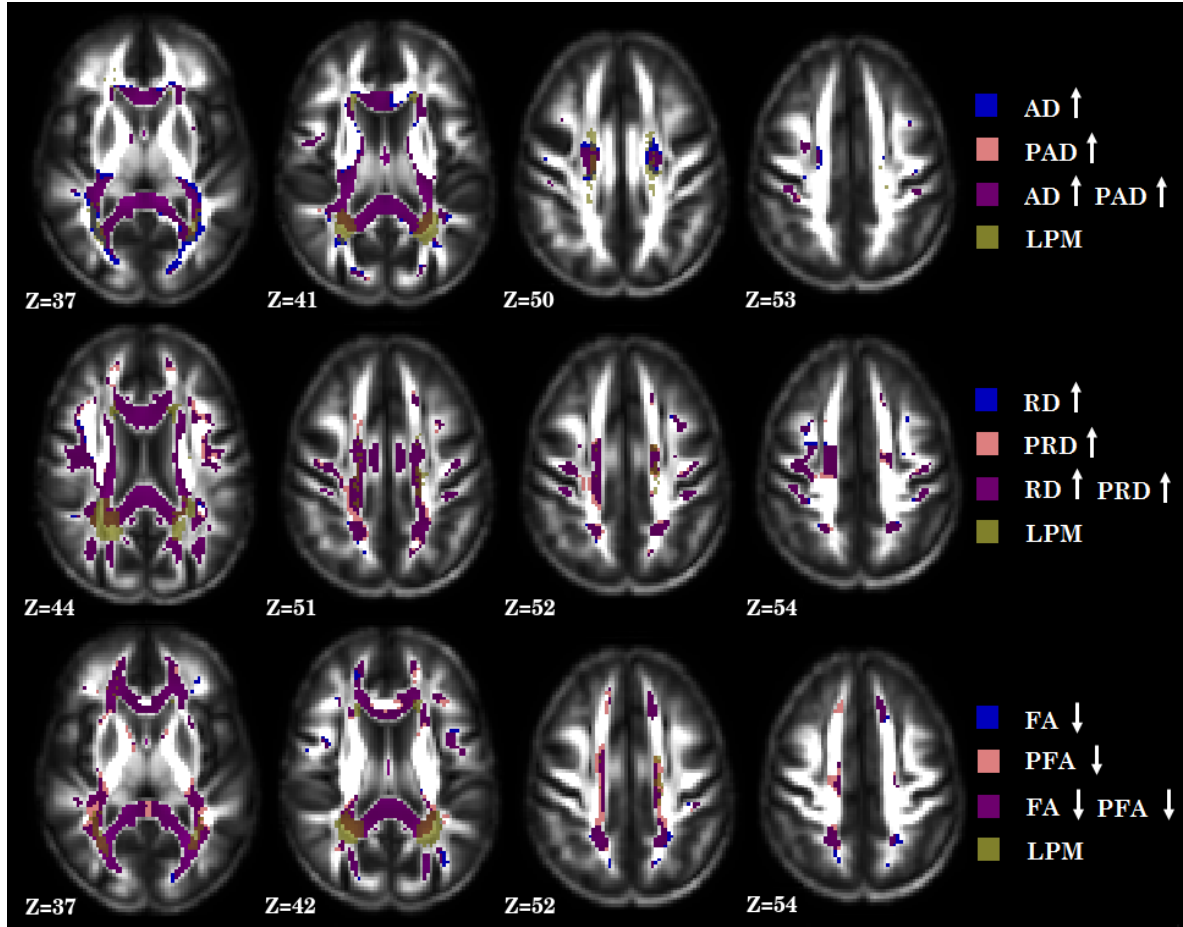


Figure 4.2: Comparison between the projected and original indices obtained with FA-based registration. Blue and pink represent areas with changes in the MS patients detected, respectively, with the standard and the projected parameters. The purple corresponds to the overlay between the blue and the pink areas while the olive green represents the LPM thresholded at 10%.

and a decrease in PFA were found in more regions than, respectively, an increase in RD and a decrease in FA. This follows the same trend as to what was observed in the DT-based registration analysis, but with more differences between the two types of parameters.

In general, the thresholded LPM overlapped with the changes detected between controls and patients. However, the regions detected with an increase of AD seem to be in better agreement with the thresholded LPM than the ones detected with an increase of PAD (Figure 4.2, slices 37, 41 and 50). On the other hand, in some voxels, the thresholded LPM overlapped with changes exclusively detected with PFA.

4.3.2 Angles analysis

By comparing the angle maps from this study and from the previous one (Chapter 3), it is visible that there is a higher dispersion between the two mean datasets using the FA-based registration.

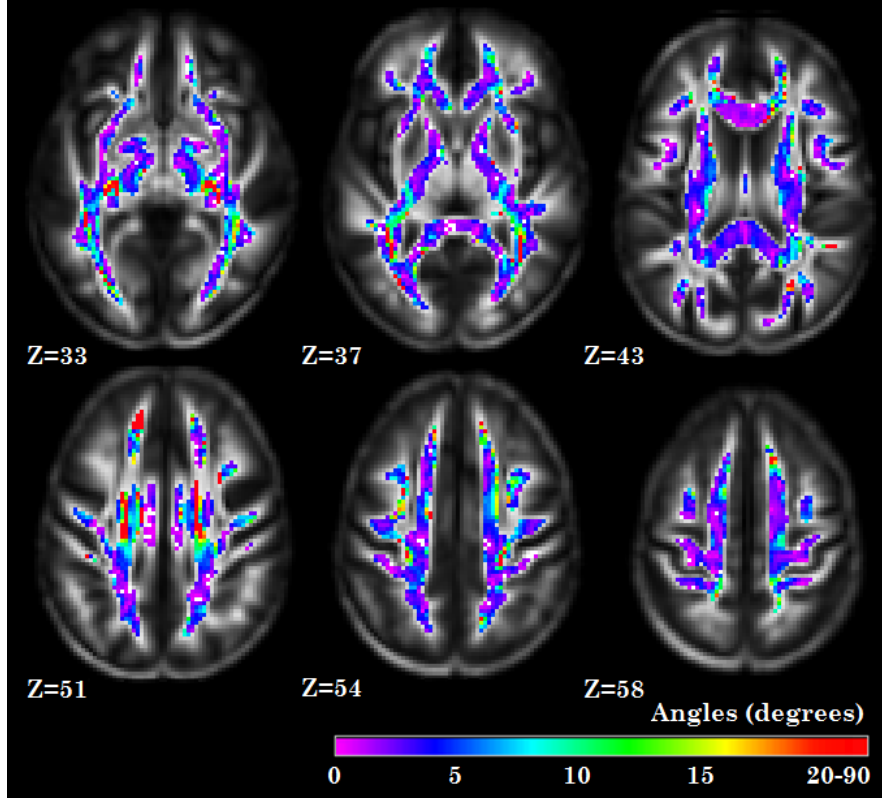


Figure 4.3: Angle between the average of MS DT-dataset and the average of HC DT-dataset obtained with FA-based registration.

In addition, the angles between the mean HC DT-datasets from the DT-based pipeline and the FA-based pipeline show differences that are due to the registration technique employed (Figure 4.4). The deviation in the principal direction of corresponding tensors is mainly below 5 degrees, however, there is also a significantly high number of voxels with greater angles. Indeed, the brightest coloured voxels seem to be localised in areas of crossing fibres or where it is expected partial volume between tissue types (e.g. white matter and ventricles or white matter and grey matter).

In addition, when observing the obtained histogram, the difference between the two registration methods is evident. These dissimilarities are quantified in Table 4.1, which show the percentage of voxels that exceed the 5 degrees in each angle analysis.

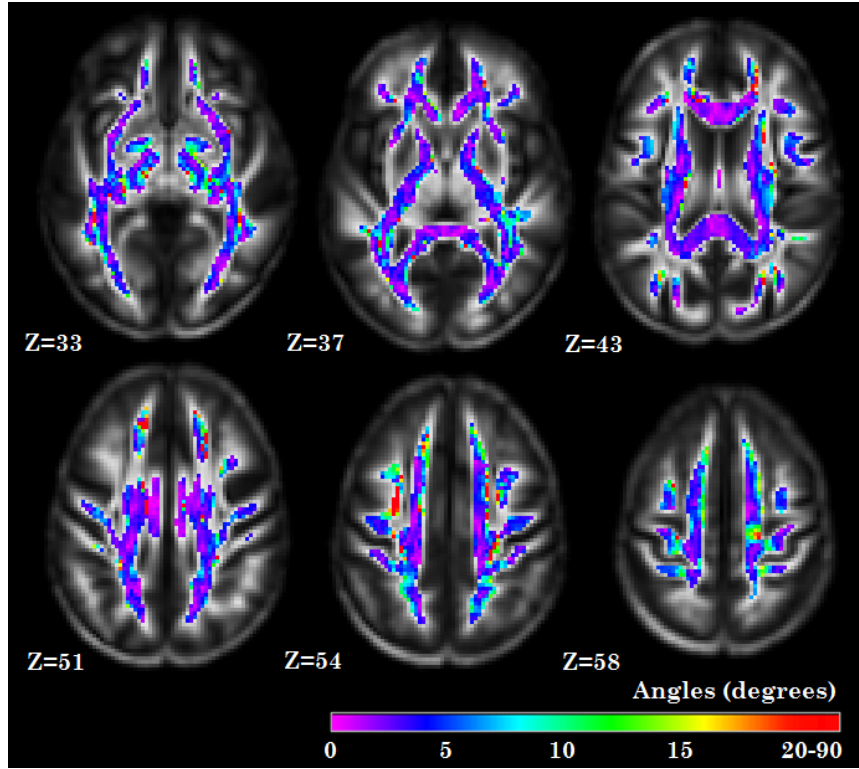


Figure 4.4: Results of the angle dispersion analysis between the mean HC DT-datasets obtained with DT-based pipeline and with FA-based pipeline.

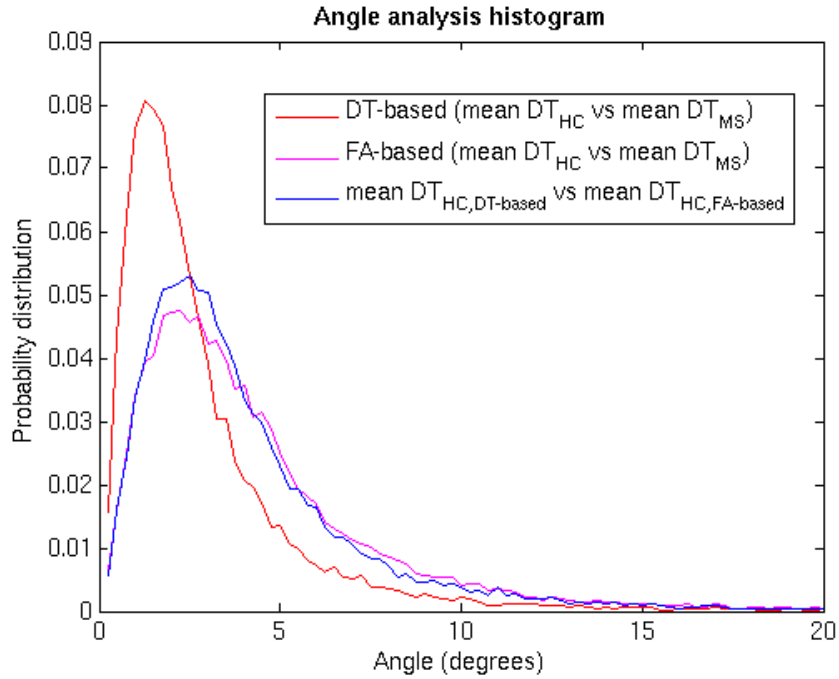


Figure 4.5: The normalized histograms show the probability of angles between 0 and 20 degrees in the white matter, for each analysis.

Table 4.1: Percentage of WM voxels with angles above 5 degrees

| Angle comparison | Percentage |
|--|------------|
| Controls and patients' mean DT-datasets (DT-based pipeline) | 13% |
| Controls and patients' mean DT-datasets (FA-based pipeline) | 29% |
| Controls' mean DT-datasets derived from DT and FA-based pipelines) | 26% |

4.4 Discussion

This analysis aimed to study whether the used registration method could significantly influence the differences in sensitivity between the projected and standard DTI indices due to patients-controls changes.

To achieve this goal, the analysis detailed in the previous study (Chapter 3) was repeated using a different registration technique, this time based on FA maps instead of DT-images, and then the results from the two analysis were compared.

First, the differences between the standard measures derived from each of the registration methods were assessed. The results obtained from the two methods presented significant differences, which were mainly perceptible for changes in AD and FA. This observation supports the importance of choosing the appropriate registration method in a VBA of DT-MRI data, specially between a DT-based or a FA-based approach.

However, the interpretation of these differences is not straightforward. The results must be interpreted with caution because the reported differences can be due to image processing biases that occur during each spatial normalization method.

The angle analysis for the DT-based registration was the one showing more orientational coherence between the datasets. The number of WM voxels with angles above 5 degrees in the angle analysis between the mean controls' datasets derived from the two registration pipelines were two times higher when compared to the results from the DT-based angle analysis. These results show the role of the DT-based pipeline in the alignment of the tensors. The orientation coherence is higher between different cohorts that are better aligned than between the same cohort that was aligned in a less precise way. This shows that there is a significantly higher dispersion in the tensors orientation across the DT-datasets registered with the FA-based method. The higher orientation dispersion in the healthy angle comparisons compared to the FA-based analysis should be due to the fact that registering the HCs with FA-based registration introduces even more variability in the orientation of the tensors.

These results are coherent with the characteristics of each registration method.

In fact, the DTI-TK algorithm has a more effective alignment, which reorients the DT fields from both controls and patients according to the template's WM orientation. However, deviations in the patients DT from the tissue microstructure due to the presence of pathology are likely to be cancelled with this registration technique. Depending on the purpose of the comparison study, this issue might be a disadvantage of using this method.

In addition, with the FA-based registration, the differences in the projected and standard approaches were more noticeable. These results are in accordance with the angle analysis. Since the FA-method presents a higher principle direction orientation dispersion between patients and controls, it is understandable that the projected parameters obtained from this registration technique differ more between the original parameters than those obtained with the DT-based registration.

It is difficult to argue what is the best way to perform the registration in DTI when there is the presence of MS pathology. Further work needs to be performed to investigate which alignment is better at preserving the pathological processes of the disease. Both post-mortem and correlation studies with clinical scores should be conducted to help answering this question. Future work could also try to assess this effect with simulation of data where differences are well characterised and can be used as reference points to assess what happens when registering data with either methods.

4.5 Conclusion

This analysis focused on studying two questions: whether the differences in sensitivity between the projected and standard DTI indices could be significantly influenced by the registration method; and the importance of the registration methodology when investigating differences in DT-derived indices between patients and healthy subjects.

The results showed that there were more differences in the changes detected between the two types of parameters using the FA-based method compared to using the DT-based one. However, it is not clear what can be interpreted from these results. Further investigation is necessary to understand whether these differences were mostly due to biases introduced by the registration technique used or to actual differences in the pathologic sensitivity of the two types of indices.

This study also showed that the two registration methods were responsible for considerable differences in the VBA analysis results. However, it is questionable whether it is the DT-based or the FA-based registration pipelines that are most adequate for comparative studies between patients and controls. Although the DT-

based registration has a better performance at aligning corresponding tensors with each other, this may not be desirable in the presence of pathology if the alignment smooths subtle changes that cause the microstructural alteration of the underlying tissue. This makes the issue of DT registration still an open topic of research that needs to be further addressed.

Chapter 5

Conclusions

5.1 Summary

In this work, challenges that come from the utilization of DTI to conduct quantitative analysis of DT-derived indices were tackled and discussed.

It was investigated whether a suggested novel approach in the literature to quantify structural integrity in the WM would be a more consistent way of comparing different groups of DT-datasets as opposed to the method currently used by the scientific community.

Due to the importance of the registration step that aligns all brain images to each other, required as the first step of this analysis, the comparison was performed for projected and standard indices derived from two different registration methods, one based on DT-images and the other based on FA maps.

This gave this study the opportunity for investigating the importance of the methodology used for the spatial normalization of the DTI images in comparative group studies between controls and patients.

5.2 Contribution

This research found that the projected parameters behave very similarly to the standard parameters when detecting regional group differences between patients and controls. However, the results also suggested that there is the possibility of a higher sensitivity in the increase of the measures PRD and PFA compared, respectively, with RD and FA.

Furthermore, the results showed that the analysis outcomes from comparative group studies can be greatly affected by the registration technique used when comparing DT-based methods with FA-based ones. It was also shown that the different

alignment algorithms between the two methods had a great influence in the coherence of the tensors orientation across the normalized DT-datasets.

Part of the work developed in this research was shared with the scientific community in a poster presentation, presented at the International Society for Magnetic Resonance in Medicine (ISMRM) Workshop on Multiple Sclerosis as a Whole-Brain Disease, held on 26-28 June 2013, in London, England, UK with the title:

Validation of the projected axial and radial diffusivities as new measures to study white matter integrity

Catarina Freitas^{1,2}, Nils Muhlert², Varun Sethi², Olga Ciccarelli³, Declan Chard³, Mara Cercignani⁴, Hui Zhang⁵, Claudia A.M. Wheeler-Kingshott² ¹*IBEB, FCUL, Lisbon, Portugal*; ²*Department of Neuroinflammation, UCL IoN, UCL*; ³*Department of Brain Repair and Rehabilitation, UCL IoN, UCL, London, UK*; ⁴*Department of Neuroscience, University of Sussex, Brighton, UK*; ⁵*Department of CS & CMIC, UCL, London, UK*.

5.3 Future work

This work on the projected indices of the diffusion tensor using different registration methods has revealed some interesting information at group level and open some further questions that make it worth pursuing the investigation of this line of research.

Namely, the pathological substrate of the projected and standard indices should be investigated with post mortem studies in order to determine which better represents MS pathology.

In addition, it is also important to study how the processing steps of the FA-based and DT-based registration methods affect the DT information regarding the pathological microstructure of the tissues and to assess which pipeline is more appropriate when conducting comparative studies between controls and patients.

5.4 Concluding remarks

It is important to consider the limitations of the DTI model to describe tissue microstructure. Measuring diffusion in the brain can give in vivo information that wouldn't be possible to acquire using other non-invasive techniques. However, the limitations and processing biases associated with DTI can result in misleading information.

This work explored the interpretation problem that can come from relating the DTI indices with the underlying tissue structure when the geometrical properties

of each subject dataset are not considered and the importance of the registration technique used to normalize the DT-datasets in comparison studies of patients and controls.

This research will be written up for publication. Furthermore, its results also led to several further questions that should be addressed in future work.

Bibliography

- [1] CA Wheeler-Kingshott, O Ciccarelli, T Schneider, DC Alexander, and M Cercignani. A new approach to structural integrity assessment based on axial and radial diffusivities. *Neuroimage*, 17(1027), 2002.
- [2] Christian Beaulieu. The basis of anisotropic water diffusion in the nervous system—a technical review. *NMR in Biomedicine*, 15(7-8):435–455, 2002.
- [3] Stewart C. Bushong. *Magnetic Resonance Imaging: Physical and Biological Principles*. Mosby Inc., 3rd edition, 2003.
- [4] Dow-Mu Koh and Harriet C. Thoeny. *Diffusion-Weighted MR Imaging: Applications in the Body*. Springer, 2010.
- [5] Q Wang, X Xu, and M Zhang. Normal aging in the basal ganglia evaluated by eigenvalues of diffusion tensor imaging. *American journal of neuroradiology*, 31(3):516–520, 2010.
- [6] Pabitra N Sen and Peter J Basser. A model for diffusion in white matter in the brain. *Biophysical journal*, 89(5):2927–2938, 2005.
- [7] Daniel C Alexander and James C Gee. Elastic matching of diffusion tensor images. *Computer Vision and Image Understanding*, 77(2):233–250, 2000.
- [8] Denis Le Bihan. Looking into the functional architecture of the brain with diffusion mri. *Nature Reviews Neuroscience*, 4(6):469–480, 2003.
- [9] S. Mori. *Introduction to Diffusion Tensor Imaging*. Elsevier Inc., 1st edition, 2007.
- [10] Paul T. Callaghan. Physics of diffusion. In Derek K. Jones, editor, *Diffusion MRI: Theory, Methods, and Applications*. Oxford University Press, 2011.
- [11] Heidi Johansen-Berg and Timothy E.J. Behrens. *Diffusion MRI: From quantitative measurement to in-vivo neuroanatomy*. Elsevier Inc., 1st edition, 2009.

BIBLIOGRAPHY

- [12] Yoshitaka Masutani, Shigeki Aoki, Osamu Abe, Naoto Hayashi, and Kuni Otomo. Mr diffusion tensor imaging: recent advance and new techniques for diffusion tensor visualization. *European journal of radiology*, 46(1):53–66, 2003.
- [13] Luis C Maas. Diffusion tensor imaging: Basic principles and emerging clinical applications. *APPLIED RADIOLOGY*, 32(6; SUPP):49–57, 2003.
- [14] Petra S Hüppi and Jessica Dubois. Diffusion tensor imaging of brain development. In *Seminars in Fetal and Neonatal Medicine*, volume 11, pages 489–497. Elsevier, 2006.
- [15] L.J. O’Donnell and C.F. Westin. An introduction to diffusion tensor image analysis. *Neurosurgery clinics of North America*, 22(1):185–96, 2001.
- [16] P. Hagmann, L. Jonasson, P. Maeder, J.P. Thiran, V.J. Wedeen, and R. Meuli. Understanding diffusion mr imaging techniques: From scalar diffusion-weighted imaging to diffusion tensor imaging and beyond. *RadioGraphics*, 26(?):?, 2006.
- [17] Derek K Jones, Mark R Symms, Mara Cercignani, and Robert J Howard. The effect of filter size on vbm analyses of dt-mri data. *Neuroimage*, 26(2):546–554, 2005.
- [18] M. Inglese and M Bester. Diffusion imaging in multiple sclerosis: research and clinical implications. *NMR in Biomedicine*, 23(7):865–872, 2010.
- [19] USA National Multiple Sclerosis Society. <http://www.nationalmssociety.org>. Accessed 20 July 2013.
- [20] adapted from Kurtzke JF. Rating neurologic impairment in multiple sclerosis: an expanded disability status scale (EDSS). *Neurology*. 1983; 33: 1444-52 University College London NHS Trust. <http://www.msdecisions.org.uk>. Accessed 13 September 2013.
- [21] WebMD. <http://www.webmd.com/multiple-sclerosis/>. Accessed 15 September 2013.
- [22] Yulin Ge, Meng Law, and Robert I. Grossman. Applications of diffusion tensor mr imaging in multiple sclerosis. *Annals of the New York Academy of Sciences*, 1064(1):202–219, 2005.
- [23] Massimo Filippi and F Agosta. Imaging biomarkers in multiple sclerosis. *Journal of Magnetic Resonance Imaging*, 31(4):770–788, 2010.

- [24] Daniel Goldberg-Zimring, Andrea UJ Mewes, Mahnaz Maddah, and Simon K Warfield. Diffusion tensor magnetic resonance imaging in multiple sclerosis. *Journal of Neuroimaging*, 15(s4):68S–81S, 2005.
- [25] Sheng-Kwei Song, Shu-Wei Sun, Michael J Ramsbottom, Chen Chang, John Russell, and Anne H Cross. Dysmyelination revealed through mri as increased radial (but unchanged axial) diffusion of water. *Neuroimage*, 17(3):1429–1436, 2002.
- [26] Sheng-Kwei Song, Jun Yoshino, Tuan Q Le, Shiow-Jiuan Lin, Shu-Wei Sun, Anne H Cross, and Regina C Armstrong. Demyelination increases radial diffusivity in corpus callosum of mouse brain. *Neuroimage*, 26(1):132–140, 2005.
- [27] Yaou Liu, Yunyun Duan, Yong He, Chunshui Yu, Jun Wang, Jing Huang, Jing Ye, Paul M. Parizel, Kuncheng Li, and Ni Shu. Whole brain white matter changes revealed by multiple diffusion metrics in multiple sclerosis: A tbss study. *European Journal of Radiology*, 81:2826–2832, 2012.
- [28] L. C. H. Cruz Jr., Raquel R. Batista, Roberto C. Domingues, and Frederik Barkhof. Diffusion magnetic resonance imaging in multiple sclerosis. *Neuroimaging Clinics of North America*, 21:71–88, 2011.
- [29] Claudia AM Wheeler-Kingshott and Mara Cercignani. About “axial” and “radial” diffusivities. *Magnetic Resonance in Medicine*, 61(5):1255–1260, 2009.
- [30] Denis Le Bihan, Cyril Poupon, Alexis Amadon, and Franck Lethimonnier. Artifacts and pitfalls in diffusion mri. *Journal of Magnetic Resonance Imaging*, 24(3):478–488, 2006.
- [31] Hui Zhang, Paul A Yushkevich, Daniel C Alexander, and James C Gee. Deformable registration of diffusion tensor mr images with explicit orientation optimization. *Medical image analysis*, 10(5):764–785, 2006.
- [32] Daniel C Alexander, Carlo Pierpaoli, Peter J Basser, and James C Gee. Spatial transformations of diffusion tensor magnetic resonance images. *Medical Imaging, IEEE Transactions on*, 20(11):1131–1139, 2001.
- [33] Dongrong Xu, Susumu Mori, Dinggang Shen, Peter van Zijl, and Christos Davatzikos. Spatial normalization of diffusion tensor fields. *Magnetic resonance in medicine*, 50(1):175–182, 2003.

- [34] H. Zhang, B.B Avants, P.A. Yushkevich, J.H. Woo, S. Wang, L.H. McCluskey, L.B. Elman, E.R. Melhem, and J.C. Gee. The high-dimensional tensor-based dti registration algorithm. *IEEE Transactions on Medical Imaging*, 26(11):1585–1597, 2007.
- [35] H. Zhang, P.A. Yushkevich, D.C. Alexander, and J.C. Gee. The original piecewise-affine tensor-based dti registration algorithm at the core of dti-tk. *Medical Image Analysis*, 10(5):764–785, 2006.
- [36] Yi Wang, Aditya Gupta, Zhexing Liu, Hui Zhang, Maria L Escolar, John H Gilmore, Sylvain Gouttard, Pierre Fillard, Eric Maltbie, Guido Gerig, et al. Dti registration in atlas based fiber analysis of infantile krabbe disease. *Neuroimage*, 55(4):1577–1586, 2011.
- [37] Stephen M Smith. Fast robust automated brain extraction. *Human brain mapping*, 17(3):143–155, 2002.
- [38] Hui Zhang, Paul A Yushkevich, Daniel Rueckert, and James C Gee. Unbiased white matter atlas construction using diffusion tensor images. In *Medical Image Computing and Computer-Assisted Intervention–MICCAI 2007*, pages 211–218. Springer, 2007.
- [39] Zhang H. http://www.nitrc.org/forum/forum.php?forum_id=1621. Accessed 13 August 2013.
- [40] Vincent Arsigny, Pierre Fillard, Xavier Pennec, and Nicholas Ayache. Log-euclidean metrics for fast and simple calculus on diffusion tensors. *Magnetic resonance in medicine*, 56(2):411–421, 2006.
- [41] Shiva Keihaninejad, Hui Zhang, Natalie S Ryan, Ian B Malone, Marc Modat, M Jorge Cardoso, David Cash, Nick C Fox, and Sebastien Ourselin. An unbiased longitudinal analysis framework for tracking white matter changes using diffusion tensor imaging with application to alzheimer’s disease. *NeuroImage*, 2013.
- [42] Andrea Mechelli, Cathy J Price, Karl J Friston, and John Ashburner. Voxel-based morphometry of the human brain: methods and applications. *Current Medical Imaging Reviews*, 1(2):105–113, 2005.
- [43] Adam W Anderson. Theoretical analysis of the effects of noise on diffusion tensor imaging. *Magnetic Resonance in Medicine*, 46(6):1174–1188, 2001.

BIBLIOGRAPHY

- [44] Derek K Jones. Determining and visualizing uncertainty in estimates of fiber orientation from diffusion tensor mri. *Magnetic Resonance in Medicine*, 49(1):7–12, 2003.

